

~~CONFIDENTIAL~~

Copy 454

RM A56111



# RESEARCH MEMORANDUM

ADDITIONAL EXPERIMENTS WITH FLAT-TOP WING-BODY  
COMBINATIONS AT HIGH SUPERSONIC SPEEDS

By Clarence A. Syvertson, Thomas J. Wong,  
and Hermilo R. Gloria

Ames Aeronautical Laboratory  
Moffett Field, Calif.

Declassified by authority of NASA  
Classification Change Notices No. 67  
Dated \*\* 6/29/66

DECLASSIFIED- AUTHORITY  
US: 1286 DROBKA TO LEBOW  
MEMO DATED 6/8/66

~~CONFIDENTIAL~~  
~~CONFIDENTIAL~~  
NATIONAL ADVISORY COMMITTEE  
FOR AERONAUTICS  
WASHINGTON

February 19, 1957

~~CONFIDENTIAL~~

## NATIONAL ADVISORY COMMITTEE FOR AERONAUTICS

RESEARCH MEMORANDUMADDITIONAL EXPERIMENTS WITH FLAT-TOP WING-BODY  
COMBINATIONS AT HIGH SUPERSONIC SPEEDSBy Clarence A. Syvertson, Thomas J. Wong,  
and Hermilo R. Gloria


## SUMMARY

An experimental study is made of the effects of several variations in configuration geometry on the aerodynamic characteristics of flat-top wing-body combinations. In general, these configurations consist of one half of a body of revolution mounted beneath a wing of essentially arrow plan form. At the root, the wing leading edge coincides with the nose of the fuselage and the trailing edge coincides with the fuselage base. Variations in model geometry studied include wing trailing-edge sweep, the addition of auxiliary bodies, downward deflection of wing tips to simulate vertical fins, wing dihedral, wing leading-edge sweep, fuselage fineness ratio, and fuselage profile shape. Lift, drag, and pitching-moment characteristics were obtained at Mach numbers from 3.00 to 6.28 and angles of attack up to  $4^\circ$ .

Many of the configurations tested were found to be relatively efficient. For example, at Mach numbers from 3 to 5, 60 percent of the maximum lift-drag ratios measured were greater than 6. The highest maximum lift-drag ratios measured were 7.2 at  $M = 3.00$  and  $M = 4.24$ , 6.6 at  $M = 5.05$ , and 5.3 at  $M = 6.28$ , although these values were not all obtained with the same configuration.

## INTRODUCTION

Several studies have been made recently to develop configurations which will be aerodynamically efficient at supersonic speeds (e.g., refs. 1 to 4). In general, these studies employed theoretical arguments in the selection of various configuration arrangements. In reference 1, this problem of designing aircraft which develop high lift-drag ratios was attacked for high supersonic speeds using an elementary principle that the components of the aircraft should be arranged to impart the maximum downward and minimum forward momentum to the surrounding air. This principle



in conjunction with other practical considerations of hypersonic flight led to the study of configurations consisting of a fuselage situated entirely beneath a wing of essentially arrow plan form. The wing leading edge at the root coincided with the nose of the fuselage and the trailing edge coincided with the fuselage base. Wing tips were deflected downward on some models, thereby simulating vertical fins.

It was estimated in reference 1 that sensibly complete aircraft of this flat-top design would develop lift-drag ratios in excess of 6 at a Mach number of 5. These estimates were, in the main, confirmed by preliminary experimental results and a maximum lift-drag ratio of 6.6 at a Mach number of 5 was obtained. By way of comparison, this value was 15 percent higher than the lift-drag ratio obtained for an entirely comparable symmetric model.

The investigation made in reference 1 was, however, of rather limited scope. The only configuration shape variables studied were wing plan form and wing-tip-flap deflection. The experimental investigation begun in reference 1 has been extended to cover several additional shape variables including fuselage fineness ratio, fuselage profile shape, wing leading-edge sweep, and the addition of auxiliary bodies. Additional investigations of wing plan form and tip-flap deflection have also been made. The effects of these variables on the aerodynamic characteristics of flat-top configurations have been determined at Mach numbers from 3.00 to 6.28. The results of these studies are the subject of the present report.

NOTATION

- $C_D$  drag coefficient,  $\frac{D}{qS}$
- $C_L$  lift coefficient,  $\frac{L}{qS}$
- $C_m$  pitching-moment coefficient,  $\frac{\text{moment about fuselage vertex}}{qS\bar{l}}$
- $C_N$  normal-force coefficient,  $\frac{\text{normal force}}{qS}$
- $D$  drag, lb
- $L$  lift, lb
- $\bar{l}$  fuselage length, in.
- $M$  Mach number
- $q$  dynamic pressure, lb/sq in.



- r fuselage radial ordinate, in.
- R Reynolds number based on fuselage length
- S total plan area of model (with tip flaps undeflected), sq in.
- x longitudinal station measured from fuselage vertex, in.
- y lateral ordinate of wing measured from configuration center line, in.
- $\alpha$  angle of attack, measured to bottom surface of wing, deg
- $\delta_c$  semivertex angle of conical fuselages, deg
- $\Gamma$  dihedral angle, deg
- $\Lambda$  sweep angle, deg
- $\theta_F$  tip-flap deflection angle, deg

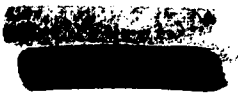
Subscripts

- b fuselage base
- max maximum

EXPERIMENT

Apparatus and Tests

Tests were conducted in the Ames 10- by 14-inch supersonic wind tunnel at Mach numbers of 3.00, 4.24, 5.05, and 6.28. A detailed description of this wind tunnel and its aerodynamic characteristics may be found in reference 5. Lift, drag, and pitching moment were measured with a three-component strain-gage balance. The balance system measured forces parallel and normal to the balance axis and these forces were, in turn, resolved to give lift and drag. Pitching moments were measured about the body base, and then, through the use of normal force, transferred to give pitching moments about the body nose. Tests were conducted at angles of attack from  $-1^\circ$  to  $+4^\circ$  by rotation of the model balance assembly. All models were sting-supported from the rear where the balance was located. The support was shrouded from the air stream to within about 0.04 inch of the model base, thereby eliminating, for all practical purposes, aerodynamic loads on the sting.





Pressures on the base of the fuselages were measured in all tests and the lift and drag components of the resultant base force (referred to free-stream static pressure) were subtracted from measured total lift and drag forces. The contribution of the base force to pitching moments was negligible.

Wind-tunnel calibration data (see, ref. 5) were employed in combination with measured stagnation pressures to obtain the stream static and dynamic pressures of the tests. Reynolds numbers (based on body length) which varied slightly due to variations in model size, were

<u>Mach number</u>	<u>Reynolds number, million</u>
3.00	4.9 to 5.4
4.24	4.4 to 4.8
5.05	2.1 to 2.4
6.28	0.9 to 1.1

Individual values for each model are presented with the respective data.

#### Models

The flat-top wing-body combinations tested in the present investigation are shown in figure 1. Pertinent geometric properties of the models, such as plan area, aspect ratio, and fuselage volume, are given in table I.

For model 1, figure 1(a), the fuselage was formed from a cone having a semivertex angle of  $5^\circ$  cut  $1^\circ$  above the axis. The wing had simple triangular plan form with  $77.4^\circ$  of leading-edge sweep. The models employing plan forms A and D in reference 1 together with model 1 form a series in which the trailing-edge sweep of the wing was progressively decreased so that ratios of total streamwise length of the wing to fuselage length were 1.4, 1.2, and 1.0, respectively.

Model 2, figure 1(b), had the same fuselage as model 1. The wing had arrow plan form and  $75^\circ$  of leading-edge sweep. This model was also tested with two auxiliary bodies in the form of pods mounted beneath the wing (see dashed lines in fig. 1(b)). Each pod was one half of a cone with a semivertex angle of  $5^\circ$ . The bases of the pods were cut off to match the wing trailing edge. The combined volume of the two pods was 23 percent of the volume of the fuselage. The center lines of the pods were aligned with the free stream and 1.250 inches outboard of the fuselage center line.




For model 3, figure 1(c), the fuselage was one half of a cone with a semivertex angle of  $7.5^\circ$ . The wing had  $75.88^\circ$  of leading-edge sweep and a modified arrow plan form. Tip flaps were formed by deflecting downward the outboard portions of the wing along streamwise hinge lines. The hinge line was located 1.250 inches (i.e., about 53.4 percent of the wing semispan) outboard of the configuration center line. Flap deflections of  $0^\circ$ ,  $15^\circ$ ,  $30^\circ$ ,  $45^\circ$ ,  $60^\circ$ , and  $75^\circ$  were tested. In addition, model 3 was tested with  $-5^\circ$  dihedral. The model fuselage was modified so that in cross section it appeared as a circular sector of  $170^\circ$  included angle. The wing was bent along its center line and mated to the wedge-shaped upper surface of the fuselage.

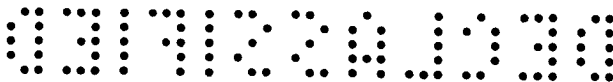
For model 4, figure 1(d), the fuselage was one half of a fineness-ratio-5 cone, semivertex angle of  $5.71^\circ$ . The wing had arrow plan form with  $80^\circ$  of leading-edge sweep. Models 5 and 6, figures 1(e) and 1(f), were similar, the primary difference being the leading-edge sweep, which was  $77.4^\circ$  and  $75^\circ$ , respectively.

The fuselages of models 7 through 10, figures 1(g) through 1(j), were one half of fineness-ratio-5 bodies of revolution. For model 7, the body was a circular-arc tangent ogive; for models 8 and 9, the bodies were defined by  $r = r_b(x/l)^n$  where  $n = 3/4$  for model 8 and  $n = 1/2$  for model 9. (The conical fuselage of model 5 may be defined in a similar manner by setting  $n = 1$ .) For model 10, the body was that which, according to impact theory, had minimum drag for the conditions of given length and volume (see, ref. 6). It may also be noted that the  $3/4$ -power body employed for model 8 closely approximates the minimum-drag body for given fineness ratio (see, ref. 6).

The wing plan forms for models 7 through 10 were selected in the following manner. A shadowgraph picture was taken of the shock wave created by the corresponding complete body of revolution at  $M = 5.05$  and  $\alpha = 0^\circ$ . As recommended in reference 1, the leading edge of the wing was designed to coincide with this shock wave. The trailing edge was formed by a straight line swept back from the base of the fuselage and intersecting the leading edge so that the total streamwise length of the wing was 1.4 body lengths. The coordinates of the fuselages and wings of models 7 through 10 are given in table II.

The leading edges of all model wings were blunt and 0.004 inch thick. All wings had a maximum thickness of 0.125 inch at the center line and the base of the fuselage. All wing sections were essentially simple wedges slightly less than 2 percent thick in streamwise planes. With the exception of model 1, the total streamwise length of all model wings was 1.4 times the body length. Models 3, 5, 7, 8, 9, and 10 were designed so that the leading edge of the wings coincided with the shock wave created by the fuselage at  $M = 5.05$  and  $\alpha = 0^\circ$ .





### Accuracy of Test Results

In the region of the test models, stream Mach numbers did not vary by more than  $\pm 0.02$  at Mach numbers of 3.00, 4.24, and 5.05. A maximum variation of  $\pm 0.04$  existed at the peak test Mach number of 6.28. Uncertainties in the angle of attack due to irregularities in the wind-tunnel air stream and to inaccuracies in the determination of the model support deflections are estimated to be  $\pm 0.1^\circ$ .

The accuracy of the test results is affected by uncertainties in the measurement of forces and moments, and in the determination of angle of attack and stream static and dynamic pressures. These uncertainties led to estimated uncertainties in the various force and moment coefficients and lift-drag ratios as shown in the following table:

M	$C_L$	$C_D$	$C_m$	L/D
3.00	$\pm 0.001$	$\pm 0.0002$	$\pm 0.001$	$\pm 0.2$
4.24	$\pm 0.001$	$\pm 0.0002$	$\pm 0.001$	$\pm 0.2$
5.05	$\pm 0.001$	$\pm 0.0002$	$\pm 0.001$	$\pm 0.2$
6.28	$\pm 0.002$	$\pm 0.0004$	$\pm 0.002$	$\pm 0.3$

It should be noted that, for the most part, the experimental results presented herein are in error by less than these estimates.

### RESULTS AND DISCUSSION

All of the experimental results obtained in the present investigation are given in table III. Lift coefficients, drag coefficients (which do not include fuselage base drag), lift-drag ratios, pitching-moment coefficients, and normal-force coefficients are given for the various test Mach numbers, Reynolds numbers, and angles of attack. It should also be noted that in the following discussion each group of test results will be considered in terms of one independent shape variable. It should not be inferred, however, that all other geometric properties are constant. For example, changes in wing leading- or trailing-edge sweep also produce changes in plan area or aspect ratio. This interdependence of the various geometric properties of the models must be kept in mind when the test results are interpreted.





## Effect of Trailing-Edge Sweep

As previously noted, two of the models tested in reference 1 in combination with model 1 of the present investigation form a series in which the wing trailing-edge sweep was progressively decreased. The trailing-edge sweep was selected so that for the model employing plan form A in reference 1, the ratio of total streamwise length of the wing to body length was 1.4. For the model employing plan form D in reference 1, the ratio was 1.2, and for model 1 of the present investigation it was 1.0. The corresponding trailing-edge sweep angles were  $60.57^\circ$ ,  $47.89^\circ$ , and  $0^\circ$ , respectively. At the four test Mach numbers of 3.00, 4.24, 5.05, and 6.28, the beginning of the expansion fan emanating from the fuselage base corresponds to sweep angles of approximately  $65^\circ$ ,  $71^\circ$ ,  $73^\circ$ , and  $75^\circ$ , respectively. For each of the three configurations, therefore, the trailing edge was always ahead of the expansion fan at all test Mach numbers. The aerodynamic characteristics of the three models at  $M = 5.05$  are compared in figure 2. Perhaps the most significant result of the comparison is that the model with plan form A (ratio of wing to body length of 1.4) has the highest maximum lift-drag ratio. The maximum lift-drag ratios of the other two models are essentially the same and about 10 percent below that of plan form A. The differences in lift-drag ratio are primarily due to differences in drag coefficients. Plan form A, which has the largest wing area, correspondingly has the lowest drag coefficients. As shown in figure 3, the model with plan form A also has the highest  $(L/D)_{\max}$  at other test Mach numbers except 6.28, where there is little difference between the three models. In view of the results shown in figures 2 and 3, all other models tested in the present investigation were constructed with a ratio of wing to body length of 1.4.

## Effect of the Addition of Auxiliary Bodies

Model 2 has been tested with and without auxiliary bodies in the form of half-cone pods mounted beneath the wing. The effect of the pods on the aerodynamic characteristics of model 2 is illustrated in figure 4 for  $M = 5.05$ . The placement of the pods beneath the wing serves to augment the lift of the configuration; however, the increase in drag more than compensates so that lift-drag ratios are decreased by the addition of the pods. Base pressures on the pods were measured, and from these measurements the base drag of the pods was determined. Drag coefficients and lift-drag ratios were then computed with the base drag of the pods subtracted from the measured drag. These results are also shown in figure 4. While removal of the pod base drag results, of course, in higher lift-drag ratios, the model with pods is still less efficient than the model without pods (fig. 4(d)). As shown in figure 5, similar results were also obtained at other test Mach numbers. The difference in  $(L/D)_{\max}$  between the model without pods and the model with pods is always less




than 10 percent if the pod base drag is removed. Under some circumstances, this difference may be a relatively small penalty for the addition of the pods, which, for example, might house auxiliary rocket motors.

### Effect of Tip-Flap Deflection

In reference 1, two models were tested with tip flaps formed by deflecting downward the outboard portions of the wing along streamwise hinge lines. The function of these flaps was, first, to deflect downward the sidewash of the body and thereby increase lift, and second, to provide surfaces for directional stability. It was found that deflection of the flaps increased the lift of the configurations at zero angle of attack but reduced lift-curve slope. The result was a net reduction in  $(L/D)_{\max}$ . The effectiveness of the flaps could be increased, it was reasoned, by increasing the sidewash over the hinge line. This possibility had been studied with model 3 of the present investigation. This model has a fuselage semivertex angle of  $7.5^\circ$  compared to  $5^\circ$  for the models of reference 1. The model was tested with flap deflections up to  $75^\circ$ , and some of the results are presented in figure 6. Characteristics of the model with flap deflections of  $0^\circ$ ,  $30^\circ$ , and  $60^\circ$ , are shown for  $M = 5.05$ . For  $\theta_F = 30^\circ$ , the loss in lift-curve slope is small, and the lift increment given by the flaps is such that the maximum lift-drag ratio is increased over that for  $\theta_F = 0^\circ$ . For  $\theta_F = 60^\circ$ , however, the loss in lift-curve slope is such that the maximum lift-drag ratio is reduced. Maximum lift-drag ratios obtained for other flap deflections and Mach numbers are shown in figure 7. It is apparent that some increase in  $(L/D)_{\max}$  was obtained with flap deflection at all test Mach numbers. Furthermore, the flap deflection for highest  $(L/D)_{\max}$  tends to increase somewhat with increasing test Mach number.

### Effect of Dihedral


As previously noted, model 3 was also tested with  $-5^\circ$  dihedral. The model was modified by removing  $5^\circ$  from the cross section on both sides of the top of the fuselage. In cross section, therefore, the fuselage appeared as a circular sector of  $170^\circ$  included angle and, thus, the frontal area and volume of the fuselage were reduced by some 5.6 percent. Correspondingly, the wing was deflected downward  $5^\circ$  on either side from the center line. The characteristics of the model with  $\Gamma = 0^\circ$  and  $\Gamma = -5^\circ$  are compared at  $M = 5.05$  in figure 8. The primary effect of the use of  $-5^\circ$  dihedral is a reduction in drag associated with the reduction in frontal area of the fuselage (fig. 8(b)). The corresponding increase in  $(L/D)_{\max}$  is about 4 percent (fig. 8(d)).



## Effect of Leading-Edge Sweep

To determine the effects of variations in wing leading-edge sweep, models 4, 5, and 6 have been tested. The fuselage for each model was one half of a fineness-ratio-5 cone (semivertex angle,  $5.71^\circ$ ). The leading-edge sweep angles were  $80^\circ$ ,  $77.4^\circ$ , and  $75^\circ$ , respectively. With these angles, the wing leading edge is designed to lie behind the body shock wave at  $M = 5.05$  for model 4, coincide with the shock wave for model 5, and lie ahead of the shock wave for model 6. The characteristics of the three models are compared in figure 9 for  $M = 5.05$ . The changes in leading-edge sweep had some effect on the lift curves (fig. 9(a)) in that the lift coefficient at  $\alpha = 0^\circ$  increased and the lift-curve slope decreased with increasing sweep. Near  $(L/D)_{\max}$  ( $\alpha \approx 3^\circ$ ), however, these effects were more or less compensating since all three models gave nearly the same lift coefficient. Drag coefficients tend to increase with increasing sweep apparently because the wing area decreased with increasing sweep while the actual drag of the fuselage remained essentially unchanged. Primarily because of this difference in drag coefficients, model 6 with the lowest leading-edge sweep gave the highest  $(L/D)_{\max}$  (fig. 9(d)). Model 6 tends to maintain this advantage over the range of test Mach numbers as shown in figure 10(a). These results, which were obtained with a fuselage semivertex angle of  $5.71^\circ$ , tend to indicate that lift-drag ratios always increase with decreasing leading-edge sweep. Actually this is not the case. For example, the model employing plan form A in reference 1 and model 2 of the present investigation can be used to demonstrate the effect of leading-edge sweep on configurations with a fuselage semivertex angle of  $5^\circ$ . For the model from reference 1, the leading-edge sweep was  $77.4^\circ$ , the same as model 5, and for model 2, it was  $75^\circ$ , the same as model 6. Maximum lift-drag ratios obtained with the two models having  $5^\circ$  fuselage semivertex angles are compared in figure 10(b). In this case it is seen that decreasing leading-edge sweep increases lift-drag ratios only at  $M = 3.00$ . At  $M = 4.24$ , it has little effect, and at  $M = 5.05$  and  $M = 6.28$ , lift-drag ratios are reduced. It would appear, therefore, that the effects of leading-edge sweep on maximum lift-drag ratio may also depend on other factors such as the fuselage shape.

It is apparent in figure 10 that for both fuselages, leading-edge sweep has its most pronounced effect on  $(L/D)_{\max}$  at the lowest test Mach number of 3.00. Both models with  $\Lambda = 75^\circ$  gave lift-drag ratios near 7; in fact, the value of 7.2 obtained with model 6 at  $M = 3.00$  (fig. 10(a)) is the highest measured in the present investigation. While this value is comparatively high, it should be noted that at this relatively low Mach number further improvement may possibly be realized by employing one of the favorable interference schemes suggested in references 2 and 3.



### Effect of Fuselage Fineness Ratio

In reference 1 and the present investigation three models were tested, each of which had a conical fuselage of different semivertex angle. Although there were some variations in wing plan form and fuselage construction, these models can be used to demonstrate some of the effects of changes in fuselage fineness ratio. The three models were that employing plan form A in reference 1, which had a fuselage semivertex angle of  $5^\circ$ , model 5 for which the angle was  $5.71^\circ$ , and model 3 for which the angle was  $7.5^\circ$ . The maximum lift-drag ratios obtained with these three models are compared in figure 11 over the range of test Mach numbers. The differences in results for the three models are less than 15 percent, of which some 5 percent may be due to the differences in plan form previously noted. The differences in lift-drag ratio are comparatively small if it is noted that the fuselage pressure drag of model 3 is approximately three times that of the model employing plan form A. In fact, some favorable effect of increasing fuselage semivertex angle was obtained at Mach numbers of 3.00 and 4.24 since model 5 gave higher  $(L/D)_{\max}$  than the model with plan form A. However, the most slender model was the most efficient at Mach numbers of 5.05 and 6.28.

### Effect of Fuselage Profile Shape

In the present investigation, configurations employing five different fuselage profile shapes were tested. In each case, the fuselage was one half of a body of revolution with a fineness ratio of 5. Each wing was designed so that the leading edge coincided with the shock wave created by the corresponding body of revolution at  $M = 5.05$  and  $\alpha = 0^\circ$ . The five configurations were model 5 and models 7 through 10. For model 5 the fuselage was conical. For model 7 the fuselage was formed from a tangent ogive. For models 8 and 9 the fuselages were formed from the bodies given by  $(r/r_b) = (x/l)^n$  where  $n = 3/4$  for model 8 and  $n = 1/2$  for model 9. For model 10 the fuselage was formed from the body of revolution which, according to impact theory (see ref. 6), had minimum pressure drag for given length and volume.

The aerodynamic characteristics of models 5, 8, and 9 are compared in figure 12 for the design Mach number of 5.05. Although model 5 with a conical fuselage has the highest lift coefficient at  $\alpha = 0^\circ$  and the highest lift-curve slope, it also has the highest drag and, as a result, the lowest maximum lift-drag ratio. The most efficient configuration is model 8 with the  $3/4$ -power fuselage. A similar comparison for models 5, 7, and 10 is made in figure 13. The two models with convex fuselages, models 7 and 10, gave essentially the same  $(L/D)_{\max}$  which was about 5 percent greater than that of model 5 with conical fuselage. Maximum lift-drag ratios obtained with all five models are compared in figure 14 over the range of test Mach numbers. At all Mach numbers, model 8 with

the 3/4-power fuselage gave the highest values of  $(L/D)_{\max}$ . Three of these values, 7.2 at  $M = 4.24$ , 6.6 at  $M = 5.05$ , and 5.3 at  $M = 6.28$ , were the highest measured at these three Mach numbers in the present investigation. By comparison, the maximum lift-drag ratios obtained with model 8 were from 6 to 15 percent higher than those obtained with model 5.

In a review of the results discussed in the foregoing sections and presented in table III and figures 2 through 14, one over-all finding becomes clearly evident. There are many flat-top configurations which will give lift-drag ratios of 6 or greater at Mach numbers between 3 and 5. In the present investigation, for example, some 17 configuration variations were tested at Mach numbers of 3.00, 4.24, 5.05, and 6.28. If the data for Mach number 6.28 are neglected due to the relatively low test Reynolds number, there remain some 51 values of maximum lift-drag ratio that were determined. Of these, 60 percent were greater than 6.0, 25 percent were greater than 6.5, and 6 percent were greater than 7.0. It is indicated, therefore, that the designer has a relatively wide latitude in selecting an efficient flat-top configuration for a particular application.

To this point, the primary emphasis of the discussion has been on the aerodynamic efficiency of the flat-top configurations. It is also interesting to consider briefly the static longitudinal stability characteristics of the test configurations, and this subject is the final topic of discussion.

#### Static Longitudinal Stability Characteristics


As indicated by data previously presented, all of the models tested displayed linear pitching-moment characteristics within the limited angle-of-attack range of the present tests. Neutral points of the flat-top configurations were, as found in reference 1, essentially invariant within the range of test Mach numbers. Since the models had no horizontal plane of symmetry, some gave finite pitching moments at zero lift. Usually these moments were small, particularly in the case of the models with conical fuselages and, where the moments did exist, they were usually positive. The existence of a positive moment at zero lift suggests the possibility that the models inherently tend to trim at some positive lift coefficient. In this event, the control moment (and associated drag penalty) required to trim the configuration at maximum lift-drag ratio would be correspondingly reduced. One of the most attractive models in this respect is model 9, which had a fuselage formed from a 1/2-power body of revolution. This model has the largest degree of nose bluntness of all test configurations. Aside from the advantage of this bluntness from the standpoint of aerodynamic heating (see, e.g., ref. 7) it also produced relatively high pressures acting on the lower surface of the wing near the nose. In turn, these pressures contributed to the positive

moment at zero lift. In order to determine the trim conditions the positive moment would give for this model a center-of-gravity location at the fuselage center of volume ( $x/l = 2/3$ ) was selected. As shown in figure 15, the neutral point for the model was between 73 and 74 percent of the body length aft of the nose at all test Mach numbers. (This location closely approximates the wing center of area at 73.4 percent.) With the center-of-gravity location selected, therefore, the static margin was approximately 6 percent of the body length. With these stability characteristics, the model was found to self-trim at lift-drag ratios greater than 6 at Mach numbers from 3 to 5 as shown in figure 15. The pitching-moment data obtained at  $M = 6.28$  were not of sufficient quality to permit an accurate determination of the trim point, and therefore trim data for  $M = 6.28$  are not shown. The results presented in figure 15 do indicate, however, that for this model trim drag penalties may have a relatively small effect on maximum lift-drag ratios.

Models 7 and 10 will also self-trim at lift-drag ratios of about 6 at Mach numbers from 3 to 5. For other models, however, self-trimmed lift-drag ratios were not so high. With a similar static margin, for example, model 8 (with the  $3/4$ -power fuselage) inherently trimmed at lift-drag ratios of about 3. For model 5 with a conical fuselage, the pitching moment at zero lift was nearly zero and the model did not trim at any appreciable lift-drag ratio. It should be emphasized, however, that these results are for the basic configurations without any control surfaces. It is possible that with the proper control surface, model 8 (with the  $3/4$ -power fuselage) may prove a more efficient trimmed configuration than model 9 (with the  $1/2$ -power fuselage), just as it proved to be the more efficient untrimmed configuration.

## CONCLUSIONS


An experimental study has been made of the effects of several variations in configuration geometry on the aerodynamic characteristics of flat-top wing-body combinations. These configurations consisted of one half of a body of revolution mounted beneath a wing of essentially arrow plan form. At the root, the wing leading edge coincided with the nose of the fuselage and the trailing edge coincided with the fuselage base. Lift, drag (not including base drag), and pitching-moment characteristics were obtained at Mach numbers from 3.00 to 6.28 and angles of attack up to  $4^\circ$ . The results of this investigation have led to the following conclusions:

1. Maximum lift-drag ratios increase with increasing wing trailing-edge sweep up to the limits of the investigation for which the length of the arrow wing was 1.4 fuselage lengths. For the models tested, the changes in lift-drag ratio were associated primarily with changes in wing area.
- 

2. Addition of auxiliary bodies beneath the wing augments the lift of a flat-top configuration; however, the drag increase is sufficient to reduce lift-drag ratios.
3. For a configuration with a conical fuselage of relatively low fineness ratio, some increase in maximum lift-drag ratio can be obtained by deflecting the wing tips downward as flaps with streamwise hinge lines.
4. Within the range from  $75^\circ$  to  $80^\circ$ , the effect of wing leading-edge sweep on maximum lift-drag ratio depends both on the free-stream Mach number and the fuselage shape. Changes in leading-edge sweep have the most pronounced effect near the lowest test Mach number of 3.00.
5. For configurations with conical fuselages, some increase in maximum lift-drag ratio is obtained by increasing fuselage semivertex angle from  $5^\circ$  to  $5.71^\circ$  at Mach numbers of 3 and 4.2. At Mach numbers of 5 and 6.3, however, the most slender fuselage tested ( $5^\circ$  semivertex angle) gives the highest maximum lift-drag ratio.
6. For configurations with fuselages consisting of one-half fineness-ratio-5 bodies of revolution, maximum lift-drag ratios are greater when the fuselage profiles are convex. Highest maximum lift-drag ratios were obtained with a model having fuselage radial ordinates proportional to the  $3/4$ -power of distance from the model nose.
7. A flat-top configuration with a relatively blunt fuselage nose can be made both stable and self-trimming. For example, one configuration tested, for which the fuselage radial ordinates are proportional to the  $1/2$ -power of distance from the model nose, inherently trims at lift-drag ratios greater than 6 with a static margin of 6-percent body length at Mach numbers from 3 to 5.

Ames Aeronautical Laboratory  
National Advisory Committee for Aeronautics  
Moffett Field, Calif., Sept. 11, 1956

#### REFERENCES

1. Eggers, A. J., Jr., and Syvertson, Clarence A.: Aircraft Configurations Developing High Lift-Drag Ratios at High Supersonic Speeds. NACA RM A55L05, 1956.
  2. Ferri, Antonio, Clarke, Joseph H., and Casaccio, Anthony: Drag Reduction in Lifting Systems by Advantageous Use of Interference. PIBAL Rept. 272, Polytechnic Institute of Brooklyn, Dept. of Aeronautical Engineering and Applied Mechanics, May 1955.
- 

0371030

3. Rossow, Vernon J.: A Theoretical Study of the Lifting Efficiency at Supersonic Speeds of Wings Utilizing Indirect Lift Induced by Vertical Surfaces. NACA RM A55L08, 1956.
4. Seiff, Alvin, and Allen, H. Julian: Some Aspects of the Design of Hypersonic Boost-Glide Aircraft. NACA RM A55E26, 1955.
5. Eggers, A. J., Jr., and Nothwang, George J.: The Ames 10-By 14-Inch Supersonic Wind Tunnel. NACA TN 3095, 1954.
6. Eggers, A. J., Jr., Resnikoff, Meyer M., and Dennis, David H.: Bodies of Revolution Having Minimum Drag at High Supersonic Airspeeds. NACA TN 3666, 1956. (Supersedes NACA RM A51K27 and RM A52D24.)
7. Goodwin, Glen: Heat-Transfer Characteristics of Blunt Two- and Three-Dimensional Bodies at Supersonic Speeds. NACA RM A55L13a, 1956.





TABLE I.- GEOMETRIC PROPERTIES OF TEST MODELS

Model	Fuselage length, in.	Plan area, sq in.	Aspect ratio	Maximum wing thickness Fuselage length	Plan area (Fuselage length) <sup>2</sup>	Fuselage volume (Fuselage length) <sup>3</sup>
Plan form A (ref. 1)	7.144	14.19	1.41	0.0175	0.278	0.00359
Plan form D (ref. 1)	7.144	12.79	1.15	.0175	.250	.00359
1	7.144	11.41	.89	.0175	.224	.00359
2	7.144	17.36	1.65	.0175	.340	.00359
2(with pods)	7.144	17.36	1.65	.0175	.340	a.00441
3	6.646	b16.20	1.35	.0188	.367	.00906
3(with -5° dihedral)	6.646	16.20	1.35	.0188	.367	.00858
4	7.144	10.56	1.17	.0175	.207	.00524
5	7.144	13.93	1.43	.0175	.273	.00524
6	7.144	17.10	1.68	.0175	.335	.00524
7	7.000	16.62	1.53	.0178	.339	.00838
8	7.000	16.47	1.48	.0178	.336	.00629
9	7.000	20.43	1.49	.0178	.417	.00786
10	7.000	17.87	1.55	.0178	.365	.00783

<sup>a</sup>Includes volume of pods.

<sup>b</sup>Flap area is 3.99 sq in. The ratio of flap area to wing area is 0.246.

TABLE II.- BODY AND WING ORDINATES FOR MODELS 7 TO 10

(a) Fuselage radial ordinates, r		(b) Wing lateral ordinates, y							
Longitudinal station	Model 7	Model 8	Model 9	Model 10	Longitudinal station	Model 7	Model 8	Model 9	Model 10
0	0	0	0	0.003	0	0	0	0	0
.10	.020	.029	.084	.039	.25	.08	.12	.22	.12
.25	.050	.058	.132	.072	.50	.15	.18	.32	.21
.50	.097	.097	.187	.119	1.00	.29	.31	.49	.37
.75	.143	.131	.229	.162	2.00	.57	.59	.80	.65
1.00	.187	.163	.264	.201	3.00	.84	.85	1.08	.92
1.50	.270	.220	.324	.271	4.00	1.10	1.09	1.35	1.18
2.00	.344	.273	.374	.335	5.00	1.36	1.33	1.60	1.43
2.50	.412	.323	.418	.392	6.00	1.61	1.57	1.85	1.68
3.00	.473	.371	.458	.445	7.00	1.85	1.81	2.09	1.93
3.50	.526	.416	.495	.494	8.00	2.09	2.05	2.33	2.18
4.00	.572	.460	.529	.537	9.00	2.33	2.29	2.57	2.43
4.50	.611	.502	.561	.578	9.80	2.52	2.47	2.76	2.63
5.00	.643	.544	.592	.616					
5.50	.668	.584	.620	.645					
6.00	.686	.623	.648	.670					
6.50	.696	.662	.675	.689					
7.00	.700	.700	.700	.700					

TABLE III.- AERODYNAMIC CHARACTERISTICS OF TEST MODELS

(a) Model 1																			
M	R, million	$\alpha$ , deg	$C_L$	$C_D$	L/D	$C_m$	$C_N$	M	R, million	$\alpha$ , deg	$C_L$	$C_D$	L/D	$C_m$	$C_N$				
3.00	5.35	-0.78	0.0032	0.0091	0.35	-0.0027	0.0031	5.05	2.32	-0.89	-0.0006	0.0063	-0.12	0.0057	-0.0007				
		-.30	.0123	.0090	1.36	-.0087	.0123			-.41	.0066	.0063	1.05	-.0005	.0065				
		.20	.0217	.0091	2.39	-.0149	.0217			.07	.0142	.0062	2.29	-.0064	.0142				
		.69	.0310	.0096	3.24	-.0211	.0311			.54	.0216	.0064	3.38	-.0130	.0217				
		1.17	.0411	.0101	4.05	-.0275	.0413			1.02	.0290	.0068	4.24	-.0181	.0292				
		1.66	.0515	.0109	4.75	-.0345	.0518			1.49	.0364	.0074	4.95	-.0231	.0366				
		2.15	.0616	.0118	5.23	-.0411	.0620			1.97	.0440	.0080	5.48	-.0290	.0443				
		2.63	.0720	.0130	5.54	-.0477	.0723			2.44	.0514	.0088	5.83	-.0345	.0517				
		3.12	.0827	.0143	5.76	-.0548	.0832			2.91	.0581	.0098	5.93	-.0388	.0585				
		3.61	.0933	.0159	5.84	-.0620	.0939			3.38	.0653	.0111	5.90	-.0438	.0659				
		4.24	4.70	-.80	-.0017	.0076	-.23			.0021	-.0018	6.28	.97	3.85	.0726	.0125	5.82	-.0488	.0732
				-.32	.0058	.0074	.78			-.0030	.0058			-1.14	.0012	.0073	.17	.0035	.0011
				.16	.0140	.0075	1.87			-.0086	.0140			-.63	.0080	.0073	1.09	.0016	.0079
				.64	.0222	.0077	2.90			-.0146	.0222			-.10	.0147	.0074	2.00	-.0038	.0147
		1.13	.0304	.0081	3.75	-.0200	.0306			.42	.0220	.0075	2.93	-.0087	.0221				
		1.62	.0384	.0087	4.40	-.0256	.0387			.94	.0291	.0079	3.69	-.0134	.0293				
		2.12	.0465	.0094	4.94	-.0310	.0469			1.47	.0363	.0086	4.23	-.0181	.0365				
		2.61	.0545	.0103	5.31	-.0365	.0549			1.99	.0434	.0092	4.73	-.0216	.0437				
		3.11	.0625	.0113	5.52	-.0419	.0631			2.52	.0503	.0101	4.97	-.0272	.0506				
		3.60	.0707	.0126	5.61	-.0475	.0714			3.05	.0570	.0112	5.13	-.0327	.0575				
										3.58	.0637	.0122	5.27	-.0371	.0644				
										4.10	.0695	.0135	5.15	-.0403	.0703				
(b) Model 2 without pods																			
3.00	5.39	-0.81	-0.0054	0.0084	-0.64	0.0032	-0.0055	5.05	2.33	-0.89	-0.0078	0.0063	-1.23	0.0108	-0.0079				
		-.31	.0060	.0083	.72	-.0048	.0059			-.41	-.0002	.0063	-.03	.0041	-.0002				
		.21	.0178	.0080	2.22	-.0141	.0178			.07	.0080	.0063	1.28	-.0030	.0080				
		.71	.0291	.0085	3.43	-.0227	.0292			.55	.0170	.0064	2.66	-.0107	.0170				
		1.21	.0409	.0091	4.51	-.0319	.0411			1.02	.0254	.0067	3.77	-.0179	.0255				
		1.71	.0531	.0098	5.44	-.0413	.0534			1.50	.0339	.0072	4.74	-.0250	.0341				
		2.21	.0659	.0107	6.17	-.0517	.0662			1.98	.0425	.0078	5.46	-.0324	.0428				
		2.71	.0780	.0118	6.60	-.0613	.0785			2.44	.0507	.0086	5.93	-.0390	.0510				
		3.21	.0902	.0131	6.86	-.0709	.0908			2.92	.0588	.0095	6.20	-.0455	.0592				
		3.72	.1043	.0150	6.97	-.0829	.1051			3.39	.0668	.0105	6.35	-.0519	.0673				
		4.24	4.72	-.81	-.0114	.0071	-1.62			.0114	-.0115	6.28	.97	-1.14	-.0044	.0081	-.54	.0098	-.0045
				-.33	-.0028	.0070	-.40			.0045	-.0029			-.63	.0023	.0080	.29	.0049	.0022
				.15	.0072	.0069	1.05			-.0038	.0072			.11	.0101	.0081	1.25	-.0019	.0101
				.65	.0173	.0070	2.47			-.0123	.0174			.42	.0177	.0082	2.15	-.0079	.0177
		1.14	.0274	.0073	3.76	-.0206	.0276			.94	.0256	.0086	2.98	-.0139	.0257				
		1.64	.0374	.0078	4.80	-.0288	.0376			1.47	.0335	.0092	3.64	-.0204	.0337				
		2.14	.0472	.0085	5.57	-.0368	.0475			2.00	.0409	.0097	4.20	-.0266	.0412				
		2.65	.0569	.0094	6.05	-.0445	.0572			2.53	.0480	.0105	4.59	-.0307	.0484				
		3.14	.0663	.0105	6.31	-.0522	.0668			3.05	.0556	.0114	4.86	-.0357	.0562				
		3.64	.0753	.0117	6.41	-.0593	.0759			3.58	.0628	.0126	4.97	-.0405	.0634				
(c) Model 2 with pods <sup>a</sup>																			
3.00	5.40	-0.78	0.0061	0.0114	0.54	-0.0065	0.0060	5.05	2.32	-0.89	-0.0006	0.0078	-0.07	0.0044	-0.0007				
		-.28	.0180	.0114	1.58	-.0155	.0179			-.41	.0076	.0078	.98	-.0035	.0076				
		.23	.0293	.0114	2.58	-.0244	.0294			.07	.0165	.0080	2.07	-.0107	.0165				
		.73	.0411	.0121	3.39	-.0338	.0413			.54	.0250	.0083	3.02	-.0180	.0251				
		1.23	.0534	.0129	4.13	-.0436	.0536			1.02	.0338	.0088	3.85	-.0253	.0340				
		1.73	.0659	.0138	4.77	-.0534	.0662			1.50	.0425	.0095	4.49	-.0327	.0427				
		2.23	.0787	.0150	5.24	-.0637	.0792			1.97	.0512	.0102	5.02	-.0401	.0515				
		2.72	.0913	.0164	5.55	-.0737	.0920			2.44	.0598	.0111	5.39	-.0472	.0602				
		3.23	.1067	.0183	5.84	-.0869	.1076			2.92	.0679	.0122	5.55	-.0537	.0685				
		3.74	.1268	.0207	6.12	-.1055	.1279			3.40	.0763	.0135	5.65	-.0609	.0770				
		4.24	4.73	-.80	-.0039	.0091	-.43			.0042	-.0040	6.28	.97	3.88	.0843	.0149	5.68	-.0673	.0882
				-.32	.0057	.0091	.63			-.0035	.0056			-1.14	.0029	.0096	.30	.0031	.0027
				.17	.0160	.0092	1.74			-.0123	.0160			-.62	.0107	.0097	1.10	-.0036	.0106
				.66	.0263	.0094	2.78			-.0207	.0264			-.10	.0189	.0099	1.90	-.0092	.0189
		1.15	.0368	.0099	3.71	-.0294	.0370			.42	.0271	.0102	2.65	-.0155	.0271				
		1.65	.0472	.0107	4.42	-.0380	.0475			.94	.0352	.0107	3.29	-.0219	.0354				
		2.14	.0572	.0116	4.95	-.0463	.0576			1.47	.0435	.0114	3.81	-.0284	.0438				
		2.65	.0670	.0127	5.29	-.0541	.0675			2.00	.0515	.0124	4.16	-.0346	.0519				
		3.15	.0767	.0140	5.47	-.0620	.0773			2.53	.0594	.0134	4.42	-.0406	.0599				
		3.65	.0858	.0155	5.55	-.0694	.0866			3.05	.0673	.0146	4.61	-.0445	.0680				
										3.59	.0757	.0161	4.70	-.0512	.0766				

<sup>a</sup>Removal of the pod base drag gives an increment in drag coefficient virtually independent of angle of attack. The increments are -0.0021 at M = 3.00, -0.0010 at M = 4.24, -0.0006 at M = 5.05, and -0.0002 at M = 6.28.

TABLE III.- AERODYNAMIC CHARACTERISTICS OF TEST MODELS - Continued

(d) Model 3, $\theta_F = 0^\circ$																			
M	R, million	$\alpha$ , deg	$C_L$	$C_D$	L/D	$C_m$	$C_N$	M	R, million	$\alpha$ , deg	$C_L$	$C_D$	L/D	$C_m$	$C_N$				
3.00	4.96	-0.75	0.0185	0.0114	1.63	-0.0137	0.0183	5.05	2.16	-0.88	0.0107	0.0084	1.27	-0.0035	0.0105				
		-.26	.0285	.0118	2.42	-.0216	.0284			-.40	.0190	.0083	2.29	-.0106	.0189				
		.24	.0394	.0121	3.24	-.0303	.0394			.08	.0278	.0084	3.30	-.0178	.0278				
		.73	.0504	.0126	3.99	-.0386	.0505			.56	.0366	.0089	4.10	-.0257	.0367				
		1.21	.0618	.0134	4.63	-.0478	.0620			1.03	.0454	.0096	4.74	-.0331	.0456				
		1.71	.0735	.0142	5.16	-.0576	.0739			1.51	.0544	.0105	5.18	-.0399	.0546				
		2.21	.0855	.0154	5.54	-.0675	.0860			1.98	.0626	.0114	5.50	-.0477	.0629				
		2.69	.0973	.0168	5.81	-.0774	.0980			2.46	.0710	.0124	5.73	-.0548	.0714				
		3.19	.1096	.0186	5.91	-.0874	.1104			2.92	.0782	.0136	5.77	-.0596	.0788				
		3.69	.1256	.0207	6.07	-.1020	.1266			3.40	.0867	.0150	5.76	-.0674	.0874				
		4.24	4.38	-.78	.0135	.0100	1.35			-.0087	.0134	6.28	.90	-1.13	.0093	.0112	.84	.0032	.0091
				-.30	.0228	.0100	2.28			-.0164	.0228			-.62	.0168	.0114	1.48	-.0034	.0165
				.18	.0326	.0102	3.20			-.0248	.0326			-.11	.0249	.0118	2.12	-.0092	.0249
				.67	.0421	.0105	4.02			-.0331	.0422			.42	.0332	.0122	2.72	-.0169	.0332
1.16	.0515			.0112	4.61	-.0405	.0517	.94	.0417	.0130	3.22			-.0240	.0419				
1.66	.0605			.0118	5.12	-.0480	.0608	1.48	.0498	.0136	3.66			-.0305	.0501				
2.15	.0701			.0127	5.50	-.0563	.0706	2.00	.0576	.0146	3.96			-.0363	.0581				
2.65	.0784			.0137	5.73	-.0631	.0790	2.53	.0654	.0156	4.19			-.0430	.0660				
3.15	.0878			.0152	5.79	-.0708	.0885	3.05	.0736	.0170	4.34			-.0498	.0744				
3.64	.0964			.0167	5.78	-.0778	.0973	3.58	.0809	.0186	4.36			-.0538	.0819				
(e) Model 3, $\theta_F = 15^\circ$																			
3.00	4.99			-0.74	0.0215	0.0111	1.93	-0.0170	0.0213	5.05	2.17			-0.88	0.0137	0.0090	1.53	-0.0068	0.0136
				-.25	.0317	.0113	2.80	-.0254	.0316					-.40	.0218	.0091	2.39	-.0133	.0217
				.24	.0422	.0118	3.58	-.0336	.0423					.08	.0303	.0092	3.29	-.0204	.0303
		.74	.0529	.0123	4.30	-.0420	.0531	.56	.0391			.0095	4.10	-.0287	.0392				
		1.23	.0643	.0131	4.92	-.0510	.0645	1.03	.0477			.0102	4.70	-.0363	.0479				
		1.72	.0758	.0140	5.42	-.0605	.0762	1.51	.0560			.0109	5.13	-.0431	.0563				
		2.21	.0877	.0152	5.77	-.0703	.0882	1.98	.0645			.0118	5.49	-.0506	.0649				
		2.70	.0994	.0166	5.99	-.0799	.1000	2.46	.0730			.0128	5.69	-.0581	.0735				
		3.19	.1121	.0183	6.12	-.0906	.1129	2.92	.0814			.0141	5.77	-.0651	.0820				
		3.70	.1294	.0205	6.31	-.1068	.1304	3.40	.0890			.0155	5.74	-.0717	.0898				
		4.24	4.40	-.78	.0162	.0101	1.60	-.0123	.0161			6.28	.90	-1.14	.0113	.0113	.99	-.0030	.0110
				-.30	.0251	.0100	2.51	-.0197	.0251					-.62	.0191	.0116	1.65	-.0103	.0190
				.18	.0347	.0102	3.41	-.0280	.0347					-.10	.0276	.0120	2.30	-.0173	.0276
				.67	.0442	.0105	4.19	-.0361	.0444					.42	.0357	.0125	2.85	-.0229	.0358
1.17	.0536			.0112	4.78	-.0438	.0538	.94	.0441	.0133	3.33			-.0288	.0443				
1.66	.0628			.0120	5.22	-.0516	.0632	1.48	.0523	.0141	3.71			-.0365	.0526				
2.15	.0721			.0129	5.58	-.0593	.0725	2.00	.0607	.0148	4.09			-.0435	.0612				
2.65	.0809			.0140	5.79	-.0666	.0815	2.53	.0688	.0160	4.31			-.0500	.0694				
3.15	.0898			.0153	5.88	-.0740	.0905	3.05	.0768	.0174	4.43			-.0567	.0777				
3.64	.0988			.0168	5.88	-.0813	.0996	3.59	.0863	.0189	4.56			-.0629	.0856				
(f) Model 3, $\theta_F = 30^\circ$																			
3.00	4.99			-0.74	0.0233	0.0114	2.05	-0.0203	0.0232	5.05	2.16			-0.88	0.0177	0.0084	2.12	-0.0089	0.0176
				-.25	.0332	.0115	2.89	-.0277	.0331					-.40	.0252	.0086	2.92	-.0152	.0252
				.24	.0432	.0120	3.61	-.0351	.0433					.08	.0340	.0090	3.78	-.0226	.0340
		.74	.0540	.0124	4.34	-.0430	.0541	.56	.0423			.0094	4.50	-.0294	.0424				
		1.23	.0652	.0133	4.92	-.0519	.0654	1.03	.0508			.0100	5.09	-.0368	.0509				
		1.72	.0765	.0142	5.41	-.0612	.0769	1.51	.0589			.0107	5.52	-.0440	.0592				
		2.21	.0882	.0153	5.75	-.0707	.0888	1.98	.0671			.0115	5.82	-.0511	.0675				
		2.70	.1001	.0167	5.98	-.0804	.1008	2.46	.0754			.0126	6.00	-.0580	.0759				
		3.19	.1118	.0184	6.08	-.0899	.1126	2.93	.0833			.0139	6.00	-.0647	.0838				
		3.70	.1274	.0205	6.23	-.1039	.1284	3.40	.0912			.0153	5.96	-.0713	.0920				
		4.24	4.39	-.78	.0182	.0099	1.83	-.0137	.0181			6.28	.90	-1.14	.0168	.0099	1.70	-.0036	.0166
				-.30	.0264	.0099	2.66	-.0203	.0264					-.62	.0236	.0104	2.27	-.0086	.0235
				.18	.0356	.0101	3.51	-.0281	.0356					-.10	.0310	.0109	2.85	-.0134	.0310
				.67	.0447	.0105	4.24	-.0359	.0448					.42	.0399	.0115	3.47	-.0219	.0400
1.17	.0537			.0112	4.80	-.0433	.0540	.94	.0477	.0123	3.89			-.0280	.0479				
1.66	.0629			.0120	5.26	-.0506	.0632	1.48	.0535	.0131	4.24			-.0343	.0558				
2.15	.0721			.0129	5.58	-.0583	.0726	2.00	.0634	.0141	4.49			-.0406	.0639				
2.65	.0810			.0141	5.75	-.0656	.0816	2.53	.0713	.0154	4.63			-.0470	.0719				
3.15	.0900			.0155	5.82	-.0731	.0907	3.05	.0793	.0168	4.71			-.0534	.0800				
3.64	.0990			.0170	5.81	-.0806	.0998	3.59	.0876	.0184	4.76			-.0604	.0886				

TABLE III. - AERODYNAMIC CHARACTERISTICS OF TEST MODELS - Continued

(g) Model 3, $\theta_F = 45^\circ$																			
M	R, million	$\alpha$ , deg	$C_L$	$C_D$	L/D	$C_m$	$C_N$	M	R, million	$\alpha$ , deg	$C_L$	$C_D$	L/D	$C_m$	$C_N$				
3.00	4.95	-0.74	0.0245	0.0110	2.24	-0.0201	0.0244	5.05	2.17	-0.88	0.0197	0.0090	2.20	-0.0109	0.0196				
		-.25	.0342	.0113	3.01	-.0276	.0341			-.40	.0275	.0092	3.00	-.0170	.0274				
		.24	.0439	.0118	3.73	-.0350	.0440			.08	.0357	.0096	3.71	-.0242	.0357				
		.74	.0539	.0123	4.37	-.0424	.0540			.56	.0438	.0101	4.35	-.0308	.0439				
		1.23	.0643	.0131	4.90	-.0505	.0645			1.03	.0521	.0108	4.85	-.0385	.0523				
		1.72	.0752	.0141	5.35	-.0592	.0756			1.51	.0600	.0115	5.21	-.0452	.0602				
		2.21	.0865	.0153	5.65	-.0683	.0870			1.98	.0676	.0123	5.11	-.0518	.0680				
		2.70	.0974	.0168	5.81	-.0770	.0981			2.46	.0757	.0132	5.72	-.0592	.0762				
		3.19	.1088	.0184	5.92	-.0862	.1097			2.93	.0837	.0145	5.77	-.0658	.0844				
		3.70	.1247	.0206	6.04	-.1007	.1258			3.40	.0914	.0159	5.75	-.0719	.0922				
		4.24	4.40	-.78	.0216	.0097	2.23			-.0176	.0214	6.28	.90	-1.14	.0177	.0106	1.67	-.0075	.0175
		-.30	.0298	.0098	3.05	-.0242	.0297			-.62	.0253			.0109	2.32	-.0155	.0252		
		.18	.0381	.0100	3.82	-.0310	.0381			-.10	.0332			.0113	2.94	-.0198	.0332		
		.67	.0473	.0105	4.52	-.0385	.0474			.42	.0409			.0116	3.54	-.0260	.0410		
		1.17	.0558	.0112	5.00	-.0452	.0560			.94	.0486			.0125	3.88	-.0320	.0488		
1.66	.0641	.0120	5.35	-.0519	.0644	1.48	.0563	.0134	4.20	-.0380	.0565								
2.15	.0728	.0130	5.62	-.0590	.0732	2.00	.0638	.0144	4.43	-.0450	.0642								
2.65	.0815	.0141	5.77	-.0660	.0821	2.53	.0718	.0155	4.62	-.0506	.0724								
3.15	.0899	.0155	5.81	-.0730	.0906	3.05	.0790	.0170	4.65	-.0561	.0797								
3.64	.0983	.0170	5.79	-.0798	.0991	3.59	.0870	.0185	4.69	-.0628	.0880								
(h) Model 3, $\theta_F = 60^\circ$																			
3.00	4.97	-0.74	0.0246	0.0111	2.22	-0.0200	0.0245	5.05	2.16	-0.87	0.0205			0.0085	2.42	-0.0129	0.0204		
		-.25	.0329	.0114	2.89	-.0258	.0328			-.40	.0270			.0086	3.16	-.0181	.0270		
		.24	.0420	.0118	3.56	-.0327	.0420			.08	.0343			.0088	3.92	-.0237	.0343		
		.74	.0508	.0124	4.11	-.0387	.0510			.56	.0414			.0093	4.44	-.0296	.0415		
		1.23	.0605	.0131	4.62	-.0459	.0608			1.03	.0487	.0099	4.92	-.0361	.0489				
		1.71	.0704	.0141	5.00	-.0534	.0708			1.51	.0560	.0107	5.23	-.0426	.0563				
		2.20	.0806	.0153	5.28	-.0611	.0811			1.98	.0629	.0115	5.48	-.0482	.0633				
		2.69	.0912	.0168	5.44	-.0693	.0919			2.46	.0706	.0125	5.64	-.0548	.0711				
		3.18	.1011	.0182	5.55	-.0768	.1019			2.92	.0779	.0138	5.63	-.0610	.0786				
		3.68	.1133	.0201	5.63	-.0869	.1143			3.40	.0851	.0153	5.57	-.0665	.0858				
		4.24	4.38	-.78	.0207	.0099	2.10			-.0166	.0206	6.28	.90	-1.14	.0195	.0100	1.95	-.0106	.0193
		-.30	.0281	.0100	2.80	-.0223	.0280			-.62	.0261			.0105	2.49	-.0144	.0260		
		.18	.0356	.0102	3.49	-.0282	.0357			-.10	.0333			.0109	3.05	-.0209	.0333		
		.67	.0434	.0107	4.07	-.0344	.0435			.42	.0409			.0115	3.55	-.0257	.0409		
		1.17	.0510	.0113	4.52	-.0402	.0512			.94	.0473			.0121	3.90	-.0304	.0475		
1.66	.0590	.0121	4.88	-.0464	.0594	1.48	.0545	.0131	4.16	-.0359	.0548								
2.15	.0668	.0130	5.13	-.0525	.0673	2.00	.0616	.0140	4.41	-.0414	.0621								
2.65	.0754	.0142	5.32	-.0589	.0755	2.53	.0687	.0152	4.52	-.0468	.0693								
3.15	.0829	.0155	5.36	-.0650	.0836	3.05	.0765	.0166	4.62	-.0541	.0773								
3.64	.0906	.0169	5.36	-.0713	.0915	3.59	.0833	.0182	4.58	-.0593	.0843								
(i) Model 3, $\theta_F = 75^\circ$																			
3.00	4.94	-0.74	0.0236	0.0113	2.09	-0.0190	0.0235	5.05	2.16	-0.88	0.0181			0.0088	2.05	-0.0097	0.0179		
		-.25	.0312	.0115	2.70	-.0238	.0311			-.40	.0240			.0091	2.65	-.0138	.0240		
		.24	.0392	.0120	3.25	-.0296	.0393			.08	.0304			.0094	3.24	-.0184	.0304		
		.73	.0473	.0125	3.77	-.0349	.0475			.56	.0367			.0098	3.76	-.0237	.0368		
		1.22	.0557	.0133	4.19	-.0405	.0560			1.03	.0430	.0103	4.17	-.0288	.0432				
		1.70	.0644	.0143	4.50	-.0465	.0648			1.51	.0494	.0109	4.55	-.0342	.0497				
		2.19	.0735	.0155	4.75	-.0532	.0741			1.98	.0559	.0117	4.80	-.0389	.0563				
		2.68	.0827	.0167	4.94	-.0598	.0834			2.46	.0621	.0127	4.89	-.0442	.0626				
		3.17	.0925	.0183	5.06	-.0669	.0933			2.92	.0686	.0138	4.96	-.0490	.0692				
		3.66	.1020	.0199	5.11	-.0741	.1030			3.40	.0749	.0151	4.96	-.0540	.0757				
		4.24	4.38	-.78	.0191	.0102	1.87			-.0146	.0190	6.28	.90	-1.14	.0173	.0109	1.58	-.0071	.0171
		-.30	.0252	.0103	2.45	-.0189	.0252			-.62	.0231			.0114	2.02	-.0100	.0230		
		.18	.0319	.0105	3.02	-.0238	.0319			-.10	.0292			.0119	2.46	-.0152	.0292		
		.67	.0386	.0109	3.53	-.0287	.0388			.42	.0357			.0124	2.89	-.0199	.0358		
		1.17	.0454	.0116	3.90	-.0337	.0456			.94	.0419			.0130	3.22	-.0232	.0421		
1.66	.0523	.0123	4.24	-.0388	.0526	1.48	.0483	.0139	3.48	-.0288	.0486								
2.15	.0591	.0132	4.47	-.0435	.0595	2.00	.0548	.0148	3.71	-.0366	.0553								
2.65	.0662	.0143	4.65	-.0489	.0668	2.53	.0613	.0160	3.84	-.0373	.0619								
3.15	.0735	.0155	4.74	-.0545	.0743	3.05	.0677	.0171	3.95	-.0420	.0685								
3.64	.0807	.0169	4.78	-.0599	.0816	3.59	.0738	.0188	3.92	-.0455	.0749								

TABLE III. - AERODYNAMIC CHARACTERISTICS OF TEST MODELS - Continued

(j) Model 3, $\Gamma = -5^\circ$																		
M	R, million	$\alpha$ , deg	C <sub>L</sub>	C <sub>D</sub>	L/D	C <sub>m</sub>	C <sub>N</sub>	M	R, million	$\alpha$ , deg	C <sub>L</sub>	C <sub>D</sub>	L/D	C <sub>m</sub>	C <sub>N</sub>			
3.00	4.96	-0.74	0.0186	0.0107	1.74	-0.0123	0.0185	5.05	2.17	-0.88	0.0117	0.0078	1.49	-0.0031	0.0115			
		-.25	.0283	.0111	2.56	-.0198	.0283			-.40	.0197	.0081	2.44	-.0092	.0196			
		.24	.0392	.0115	3.41	-.0285	.0393			.08	.0286	.0084	3.41	-.0172	.0286			
		.73	.0503	.0120	4.20	-.0378	.0504			.56	.0374	.0088	4.24	-.0254	.0375			
		1.23	.0617	.0127	4.86	-.0472	.0620			1.03	.0461	.0092	4.99	-.0332	.0463			
		1.72	.0735	.0137	5.38	-.0568	.0739			1.51	.0548	.0099	5.55	-.0405	.0551			
		2.21	.0855	.0148	5.77	-.0667	.0860			1.98	.0634	.0110	5.78	-.0477	.0637			
		2.71	.0974	.0162	6.01	-.0764	.0980			2.45	.0716	.0120	5.94	-.0540	.0720			
		3.19	.1095	.0178	6.14	-.0865	.1103			2.93	.0796	.0133	6.00	-.0607	.0802			
		3.70	.1267	.0200	6.33	-.1025	.1277			3.40	.0875	.0146	5.99	-.0675	.0882			
		4.24	4.42	-.78	.0143	.0071	2.03			-.0099	.0142	3.88	.0951	.0163	5.85	-.0736	.0960	
				-.30	.0195	.0095	2.06			-.0129	.0194							
				.18	.0290	.0096	3.02			-.0208	.0290							
				.67	.0386	.0101	3.84			-.0285	.0387							
				1.16	.0480	.0106	4.51			-.0369	.0482							
				1.65	.0575	.0115	5.02			-.0450	.0578							
				2.14	.0671	.0124	5.40			-.0531	.0675							
				2.65	.0764	.0136	5.64			-.0608	.0769							
		3.15	.0855	.0149	5.74	-.0687	.0862											
		3.64	.0942	.0164	5.76	-.0758	.0951											
(k) Model 4																		
3.00	5.35	-0.97	0.0071	0.0089	.80	-0.0014	0.0070	5.05	2.34	-1.09	0.0060	0.0071	0.85	-0.0107	0.0059			
		0	.0239	.0093	2.56	-.0153	.0239			-.13	.0207	.0070	2.96	-.0196	.0207			
		.96	.0429	.0100	4.27	-.0307	.0430			.81	.0364	.0075	4.85	-.0316	.0365			
		1.92	.0620	.0115	5.40	-.0462	.0624			1.77	.0500	.0088	5.66	-.0413	.0503			
		2.40	.0715	.0126	5.69	-.0537	.0719			2.22	.0554	.0096	5.75	-.0442	.0557			
		2.88	.0806	.0136	5.92	-.0611	.0812			2.70	.0617	.0108	5.73	-.0480	.0621			
		3.36	.0901	.0150	6.02	-.0694	.0908			3.17	.0674	.0119	5.64	-.0519	.0680			
		3.84	.0993	.0165	6.02	-.0759	.1002			6.28	0.99	-1.34	.0037	.0098	.38	-.0080	.0035	
		4.24	4.76	-1.00	.0067	.0071	.94			-.0052	.0065	-.32	.0175	.0098	1.78	-.0201	.0174	
				-.04	.0214	.0072	2.99			-.0173	.0214	.73	.0300	.0106	2.84	-.0290	.0302	
				.93	.0379	.0080	4.71			-.0311	.0380	1.79	.0439	.0116	3.80	-.0391	.0442	
				1.90	.0522	.0093	5.59			-.0430	.0525	2.32	.0508	.0123	4.13	-.0444	.0513	
		2.39	.0606	.0103	5.90	-.0499	.0610	2.84	.0600	.0134	4.50	-.0507	.0606					
		2.89	.0689	.0114	6.03	-.0562	.0694	3.37	.0657	.0146	4.51	-.0546	.0665					
		3.38	.0754	.0126	6.01	-.0612	.0760											
(l) Model 5																		
3.00	5.36	-0.99	0.0027	0.0085	0.32	-0.0019	0.0025	5.05	2.32	-1.08	-0.0021	0.0065	-.33	0.0022	-0.0023			
		0	.0239	.0086	2.77	-.0191	.0239			-.13	.0142	.0065	2.19	-.0105	.0142			
		.97	.0455	.0095	4.76	-.0366	.0456			.82	.0312	.0071	4.36	-.0241	.0313			
		1.94	.0681	.0112	6.08	-.0548	.0684			1.77	.0483	.0084	5.74	-.0378	.0486			
		2.43	.0794	.0123	6.45	-.0638	.0799			2.24	.0564	.0094	6.02	-.0439	.0567			
		2.92	.0907	.0136	6.67	-.0730	.0912			2.72	.0635	.0104	6.09	-.0492	.0639			
		3.40	.1018	.0152	6.71	-.0810	.1026			3.18	.0703	.0117	6.02	-.0542	.0708			
		3.89	.1129	.0169	6.70	-.0900	.1138			6.28	1.00	-1.34	-.0034	.0091	-.37	-.0008	-.0036	
		4.24	4.76	-1.00	-.0005	.0069	-.07			0	-.0006	-.32	.0132	.0091	1.44	-.0142	.0131	
				-.04	.0189	.0069	2.75			-.0162	.0189	.74	.0279	.0099	2.81	-.0257	.0280	
				.94	.0384	.0077	4.97			-.0323	.0385	1.79	.0427	.0112	3.80	-.0367	.0430	
				1.91	.0568	.0092	6.16			-.0473	.0571	2.32	.0505	.0121	4.16	-.0430	.0509	
				2.41	.0656	.0102	6.44			-.0543	.0660	2.84	.0582	.0131	4.44	-.0491	.0587	
				2.91	.0739	.0113	6.54			-.0610	.0744	3.37	.0650	.0143	4.54	-.0534	.0658	
		3.40	.0820	.0127	6.48	-.0668	.0826											

TABLE III.- AERODYNAMIC CHARACTERISTICS OF TEST MODELS - Continued

(m) Model 6																			
M	R, million	$\alpha$ , deg	C <sub>L</sub>	C <sub>D</sub>	L/D	C <sub>m</sub>	C <sub>N</sub>	M	R, million	$\alpha$ , deg	C <sub>L</sub>	C <sub>D</sub>	L/D	C <sub>m</sub>	C <sub>N</sub>				
3.00	5.36	-1.00	-0.0052	0.0084	-0.62	0.0050	-0.0054	5.05	2.32	-1.09	-0.0083	0.0066	-1.25	0.0070	-0.0084				
		.01	.0209	.0082	2.55	-.0162	.0209			-.13	.0086	.0064	1.35	-.0057	.0086				
		.99	.0455	.0093	4.91	-.0361	.0456			.82	.0266	.0070	3.83	-.0206	.0267				
		1.98	.0717	.0110	6.52	-.0568	.0721			1.77	.0446	.0082	5.46	-.0343	.0448				
		2.47	.0852	.0122	6.98	-.0675	.0856			2.24	.0534	.0090	5.95	-.0412	.0537				
		2.97	.0983	.0136	7.21	-.0782	.0989			2.71	.0619	.0100	6.20	-.0477	.0623				
		3.47	.1107	.0153	7.24	-.0878	.1114			3.19	.0702	.0111	6.32	-.0543	.0708				
		3.96	.1227	.0172	7.14	-.0971	.1236			6.28	1.00	-1.34	-.0091	.0088	-1.03	.0059	-.0093		
		4.24	4.74	-1.01	-.0081	.0066	-1.24					.0077	-.0082	-.32	.0071	.0087	.82	-.0074	.0071
		-.04		.0129	.0065	1.97	-.0102					.0129	.74	.0227	.0090	2.52	-.0199	.0228	
.94	.0340	.0072		4.70	-.0276	.0341	1.79	.0382	.0104			3.69	-.0320	.0385					
1.93	.0547	.0086		6.39	-.0448	.0550	2.32	.0460	.0112			4.10	-.0379	.0464					
2.43	.0643	.0095		6.74	-.0525	.0646	2.84	.0537	.0124			4.31	-.0440	.0542					
2.93	.0740	.0107		6.91	-.0603	.0744	3.38	.0621	.0133			4.67	-.0507	.0628					
3.42	.0837	.0121		6.89	-.0686	.0842													
(n) Model 7																			
3.00	5.18	-1.21		-0.0148	0.0082	-1.80	0.0177	-0.0149	5.05			2.28	-1.20	-0.0072	0.0058	-1.24	0.0098	-0.0074	
		-.16		.0065	.0085	.77	.0014	.0065		-.19	.0088		.0057	1.55	-.0029	.0088			
		.89	.0292	.0087	3.38	-.0166	.0294	.82		.0245	.0061		4.00	-.0149	.0247				
		1.94	.0523	.0098	5.34	-.0349	.0526	1.83		.0395	.0070		5.62	-.0265	.0397				
		2.46	.0636	.0107	5.95	-.0440	.0640	2.34		.0466	.0077		6.07	-.0318	.0469				
		2.99	.0745	.0117	6.39	-.0524	.0750	2.84		.0541	.0086		6.30	-.0375	.0544				
		3.51	.0856	.0130	6.58	-.0604	.0862	3.35		.0606	.0095		6.36	-.0425	.0610				
		4.04	.0959	.0145	6.61	-.0688	.0967	3.85		.0674	.0107		6.28	-.0475	.0680				
		4.24	4.63	-1.20	-.0091	.0068	-1.35	.0126		-.0093	6.28		.97	-1.20	-.0040	.0076	-.53	-.0047	-.0042
				-.18	.0087	.0064	2.11	-.0016		.0087				-.20	.0097	.0080	1.21	-.0057	.0096
.84	.0262			.0069	3.81	-.0156	.0262	.81	.0245	.0088		2.80		-.0177	.0247				
1.86	.0430			.0079	5.44	-.0289	.0432	1.81	.0395	.0103		3.85		-.0288	.0398				
2.37	.0511			.0086	5.96	-.0353	.0514	2.31	.0462	.0111		4.18		-.0341	.0466				
2.88	.0590			.0094	6.25	-.0416	.0593	2.82	.0526	.0120		4.38		-.0389	.0531				
3.39	.0667			.0105	6.35	-.0477	.0672	3.32	.0590	.0130		4.54		-.0432	.0597				
(o) Model 8																			
3.00	5.22			-1.21	-0.0089	0.0078	-1.13	0.0097	-0.0090	5.05		2.29		-1.20	-0.0076	0.0052	-1.47	0.0080	-0.0077
				-.16	.0124	.0073	1.71	-.0066	.0124					-.19	.0077	.0051	1.49	-.0035	.0076
		.88	.0336	.0081	4.17	-.0232	.0338	.82	.0232		.0057		4.09	-.0152	.0233				
		1.93	.0565	.0092	6.12	-.0404	.0567	1.83	.0396		.0067		5.94	-.0270	.0398				
		2.46	.0676	.0101	6.72	-.0482	.0680	2.34	.0469		.0074		6.38	-.0333	.0472				
		2.98	.0789	.0113	7.00	-.0578	.0794	2.84	.0542		.0082		6.60	-.0386	.0546				
		3.51	.0893	.0126	7.11	-.0652	.0899	3.35	.0609		.0092		6.63	-.0431	.0613				
		4.24	4.64	-1.21	-.0075	.0063	-1.18	.0077	-.0076		6.28		.95	-1.20	-.0048	.0072	-.67	.0006	-.0050
				-.18	.0108	.0060	1.81	-.0062	.0108					-.20	.0092	.0073	1.26	-.0098	.0092
				.84	.0291	.0063	4.66	-.0206	.0292					.81	.0240	.0078	3.07	-.0215	.0241
1.86	.0441			.0072	6.14	-.0319	.0443	1.81	.0386	.0089		4.33		-.0325	.0389				
2.37	.0547			.0080	6.85	-.0402	.0550	2.31	.0462	.0097		4.76		-.0381	.0466				
2.89	.0626			.0088	7.09	-.0463	.0631	2.81	.0532	.0104		5.10		-.0435	.0537				
3.40	.0704			.0098	7.20	-.0518	.0709	3.32	.0610	.0116		5.27		-.0498	.0616				



TABLE III.- AERODYNAMIC CHARACTERISTICS OF TEST MODELS - Concluded

(p) Model 9																	
M	R, million	$\alpha$ , deg	$C_L$	$C_D$	L/D	$C_m$	$C_N$	M	R, million	$\alpha$ , deg	$C_L$	$C_D$	L/D	$C_m$	$C_N$		
3.00	5.17	-1.24	-0.0180	0.0079	-2.26	0.0169	-0.0178	5.05	2.28	-1.20	-0.0095	0.0059	-1.60	0.0105	-0.0096		
		-.17	.0047	.0074	.64	.0006	.0047			-.19	.0062	.0058	1.07	-.0012	.0062		
		.90	.0273	.0080	3.40	-.0159	.0275			.82	.0218	.0061	3.61	-.0128	.0220		
		1.97	.0511	.0091	5.61	-.0335	.0514			1.84	.0367	.0068	5.38	-.0235	.0369		
		2.50	.0630	.0100	6.33	-.0422	.0634			2.34	.0438	.0074	5.92	-.0283	.0440		
		3.04	.0739	.0110	6.75	-.0500	.0744			2.85	.0513	.0082	6.29	-.0339	.0517		
		3.57	.0851	.0124	6.87	-.0580	.0857			3.36	.0584	.0090	6.45	-.0397	.0588		
		4.24	4.65	-1.21	-.0123	.0064	-1.92			.0129	-0.0125	-1.20	-.0039	.0077	-.51	.0021	-.0040
		-.18	.0058	.0061	.96	-.0007	.0058			-.20	.0097	.0078	1.24	-.0074	.0097		
		.85	.0238	.0063	3.78	-.0141	.0239			.81	.0238	.0083	2.87	-.0180	.0240		
1.88	.0408	.0072	5.66	-.0268	.0410	1.81	.0374	.0092	4.08	-.0274	.0376						
2.39	.0491	.0078	6.27	-.0330	.0494	2.32	.0448	.0097	4.61	-.0335	.0451						
2.90	.0573	.0087	6.58	-.0391	.0577	2.82	.0515	.0105	4.93	-.0384	.0520						
3.42	.0653	.0097	6.74	-.0450	.0658	3.32	.0588	.0113	5.19	-.0437	.0594						
(q) Model 10																	
3.00	5.21	-1.22	-0.0128	0.0078	-1.64	0.0139	-0.0130	5.05	2.29	-1.20	-0.0078	0.0061	-1.27	0.0087	-0.0079		
		-.16	.0093	.0075	1.25	-.0028	.0093			-.19	.0092	.0060	1.54	-.0041	.0092		
		.89	.0319	.0082	3.89	-.0197	.0320			.82	.0259	.0066	3.95	-.0166	.0260		
		1.95	.0555	.0094	5.88	-.0376	.0558			1.83	.0418	.0076	5.49	-.0284	.0420		
		2.48	.0671	.0104	6.43	-.0463	.0675			2.34	.0495	.0083	5.99	-.0341	.0498		
		3.01	.0787	.0117	6.73	-.0553	.0792			2.85	.0570	.0091	6.30	-.0395	.0574		
		3.53	.0898	.0130	6.89	-.0631	.0904			3.35	.0641	.0101	6.38	-.0452	.0646		
		4.24	4.66	-1.21	-.0092	.0064	-1.44			.0103	-.0093	-1.20	-.0038	.0088	-.43	.0007	-.0039
		-.18	.0097	.0061	1.60	-.0041	.0096			-.20	.0111	.0089	1.25	-.0105	.0110		
		.84	.0282	.0065	4.37	-.0183	.0283			.81	.0258	.0095	2.73	-.0194	.0260		
1.87	.0457	.0076	6.05	-.0315	.0459	1.81	.0400	.0103	3.87	-.0288	.0403						
2.38	.0540	.0083	6.52	-.0377	.0543	2.32	.0484	.0111	4.35	-.0354	.0488						
2.89	.0623	.0092	6.77	-.0440	.0627	2.82	.0560	.0120	4.67	-.0416	.0566						
3.40	.0703	.0103	6.86	-.0499	.0708	3.32	.0631	.0129	4.90	-.0463	.0637						

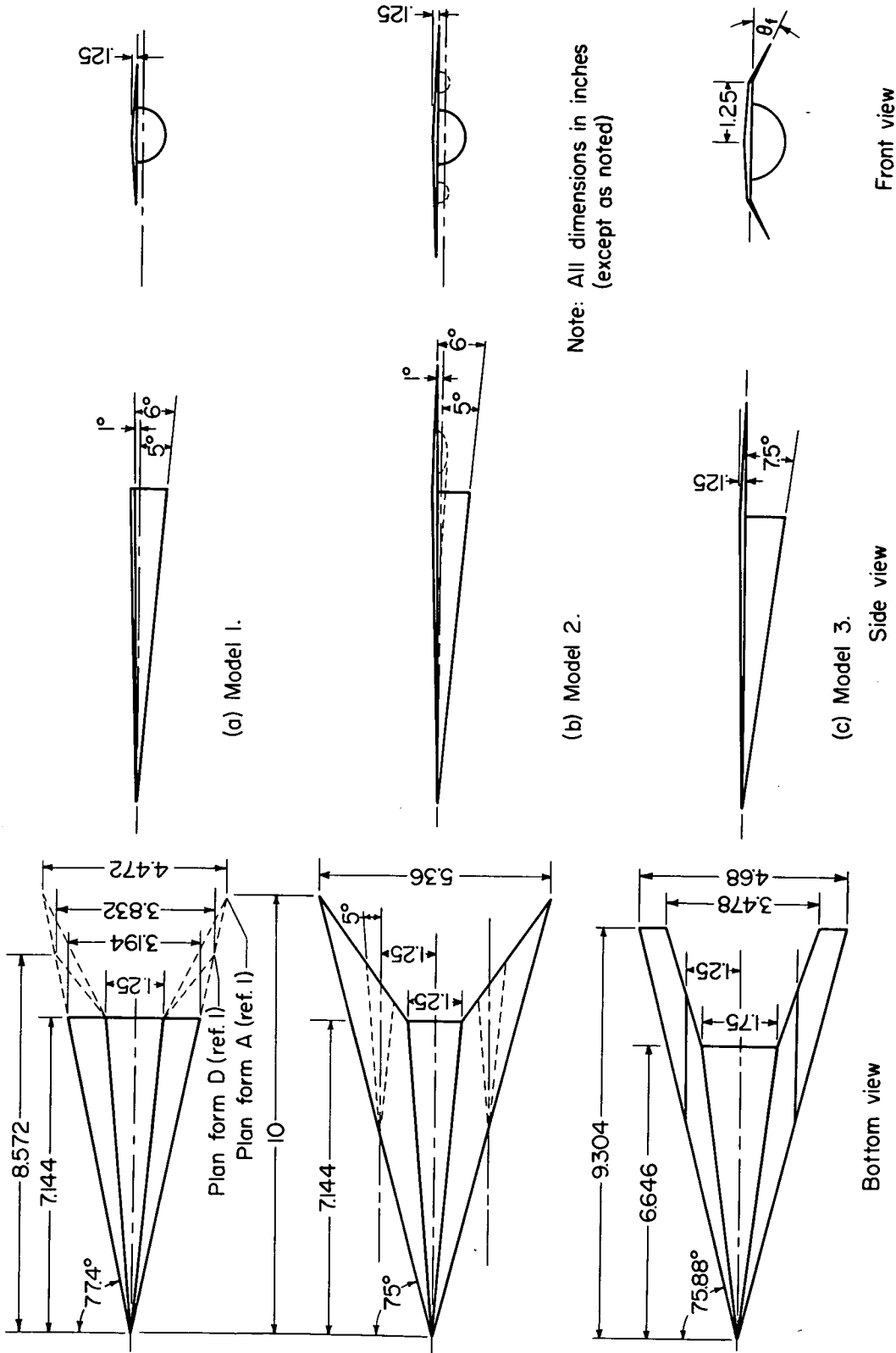


Figure 1.- Test models.

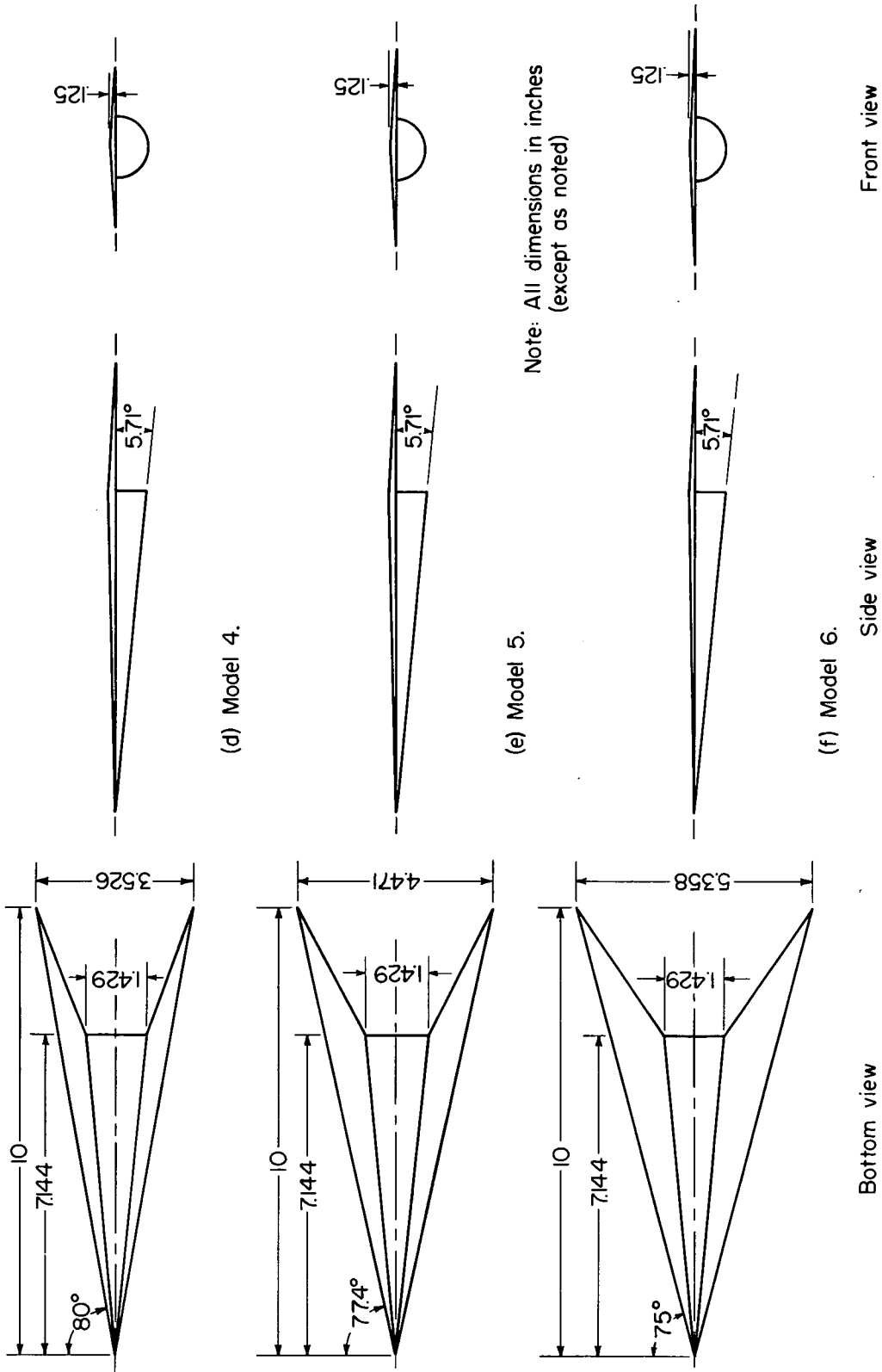


Figure 1.- Continued.

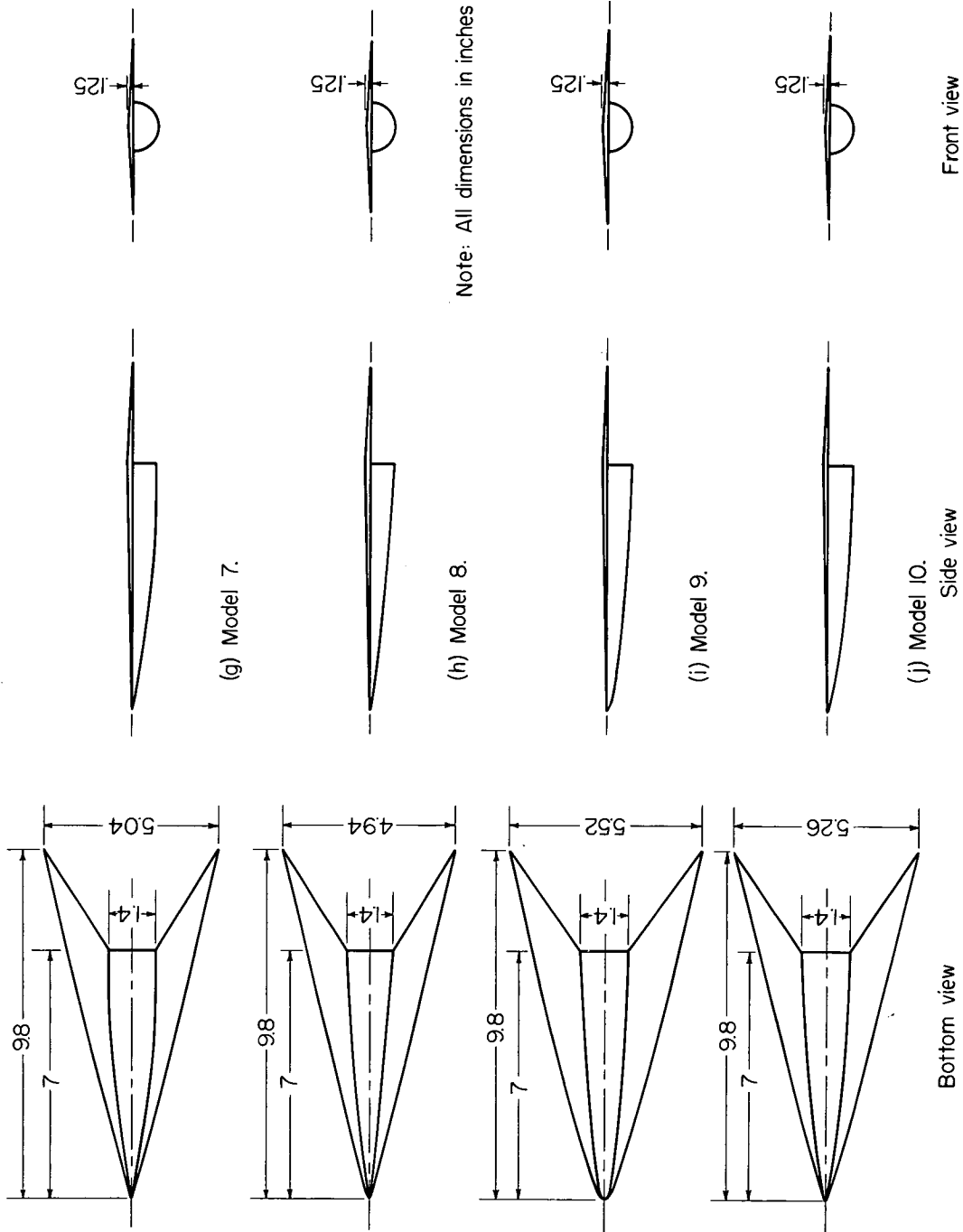
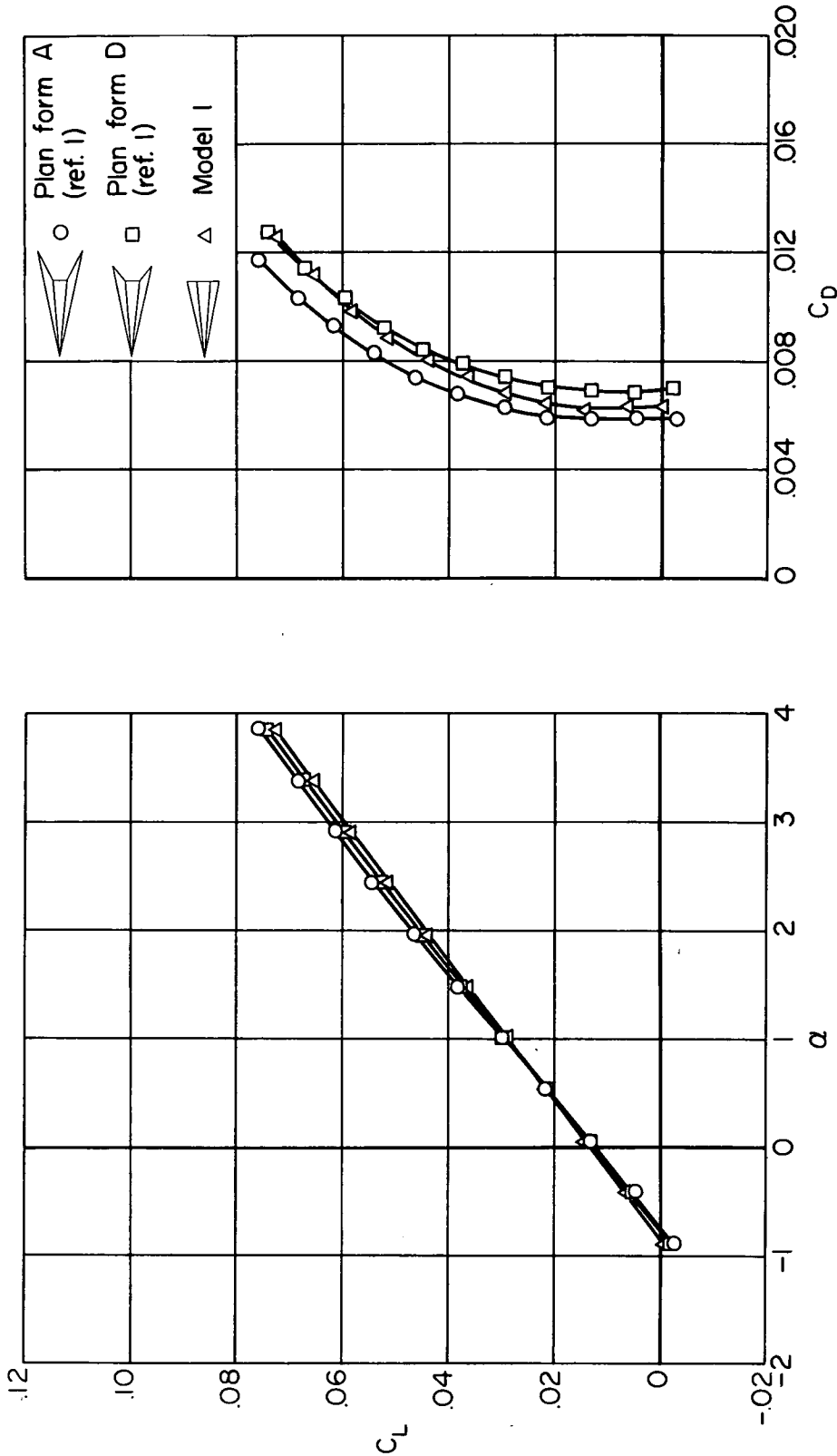


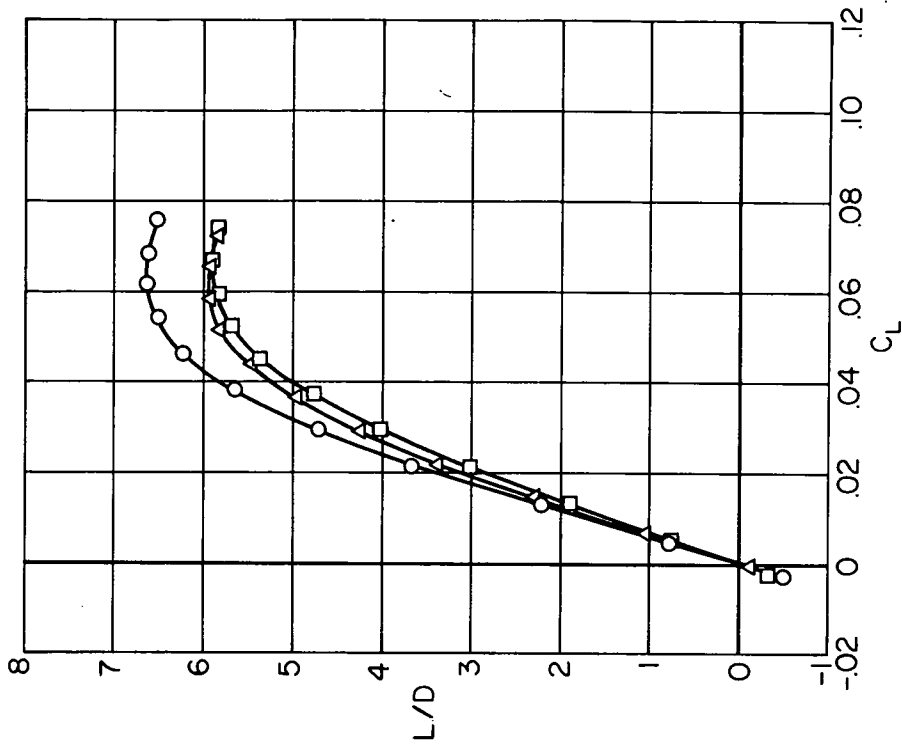
Figure 1.- Concluded.



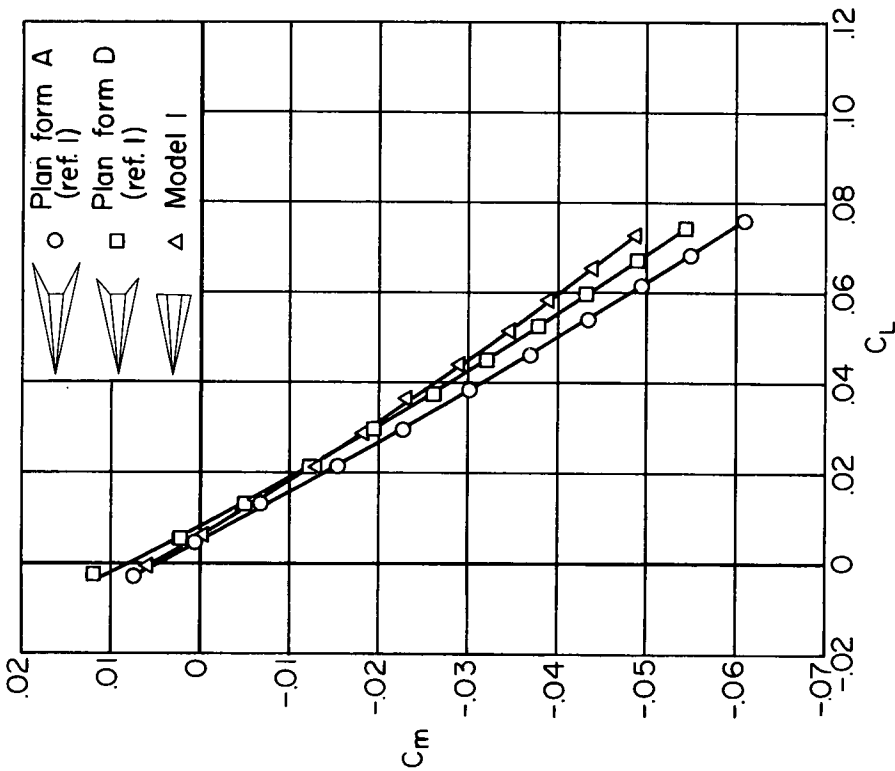
(a) Lift curve.

(b) Drag polar.

Figure 2.- Effect of trailing-edge sweep on the aerodynamic characteristics of flat-top wing-body combinations at  $M = 5.05$ .



(d) Lift-drag ratio.



(c) Longitudinal stability.

Figure 2.- Concluded.

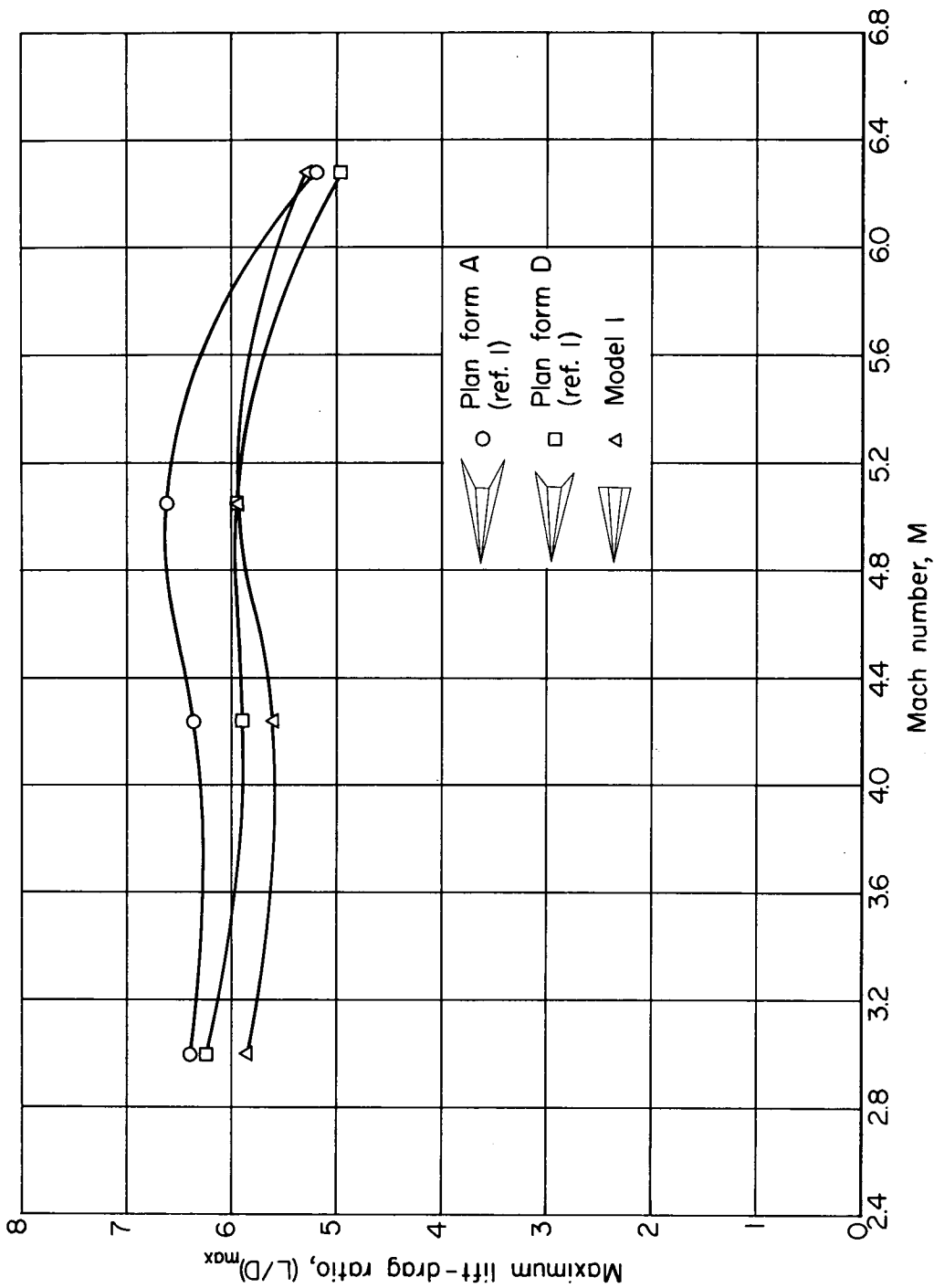


Figure 3.- Effect of trailing-edge sweep on maximum lift-drag ratios.



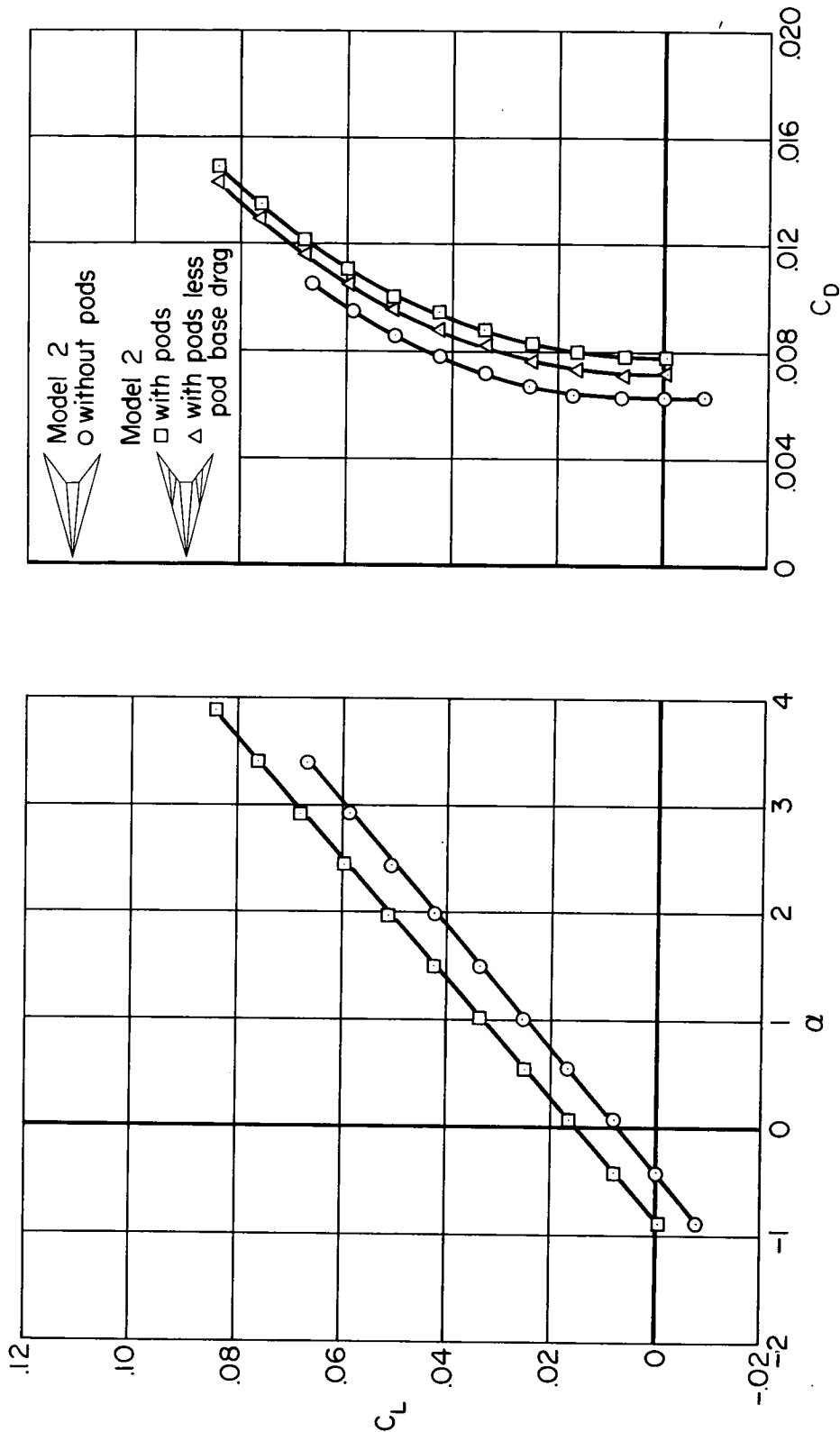
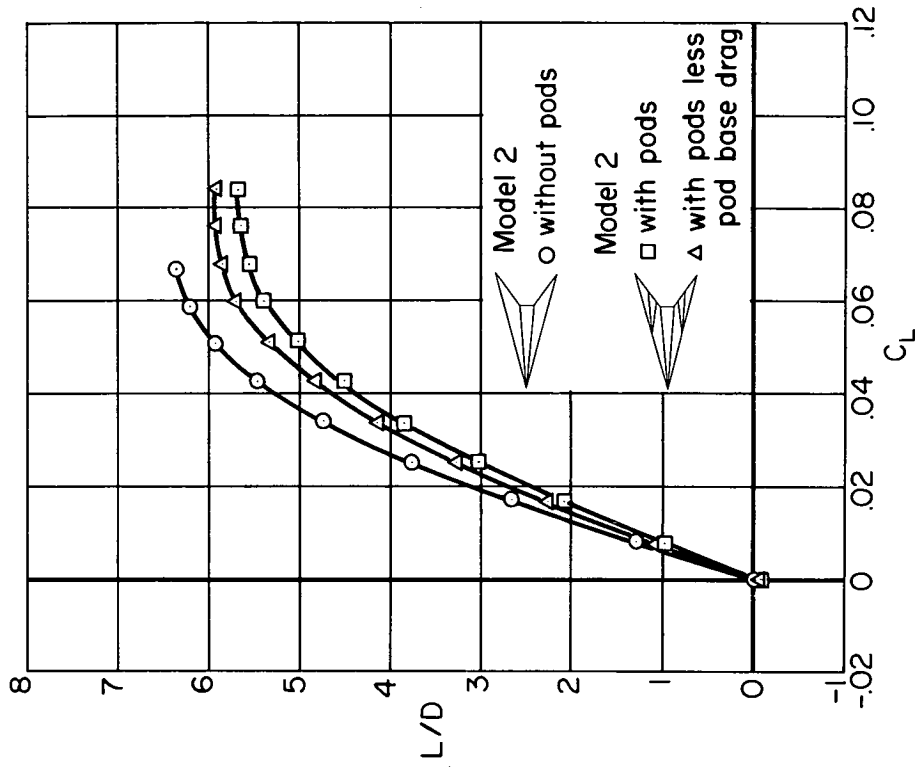
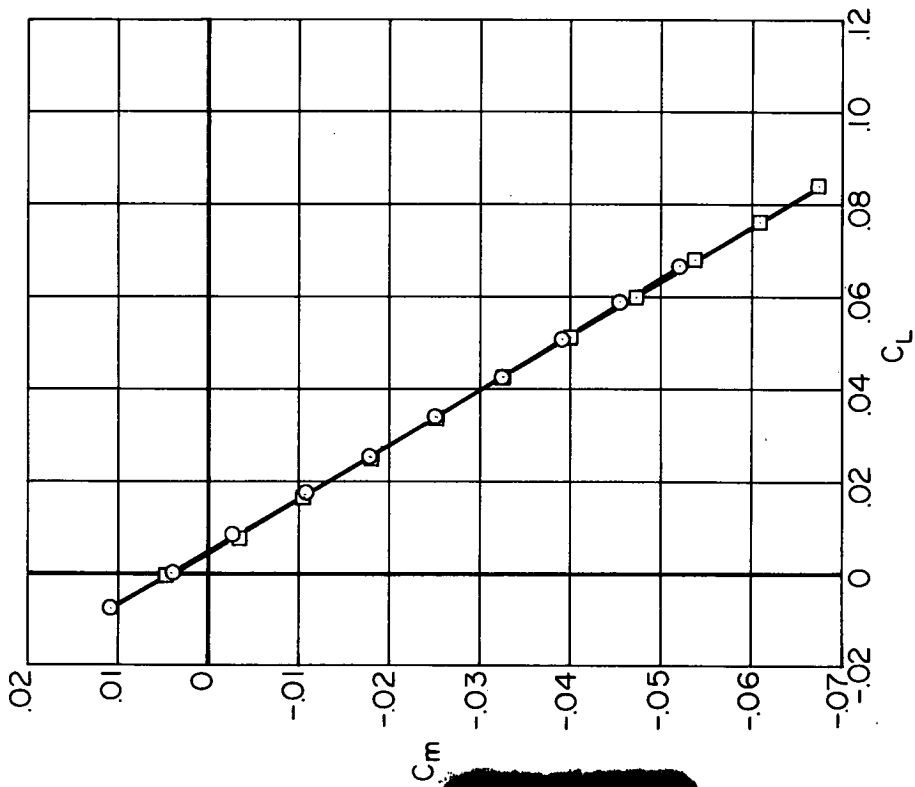


Figure 4.- Effect of the addition of auxiliary bodies on the aerodynamic characteristics of flat-top wing-body combinations at  $M = 5.05$ .



(d) Lift-drag ratio.



(c) Longitudinal stability.

Figure 4.- Concluded.

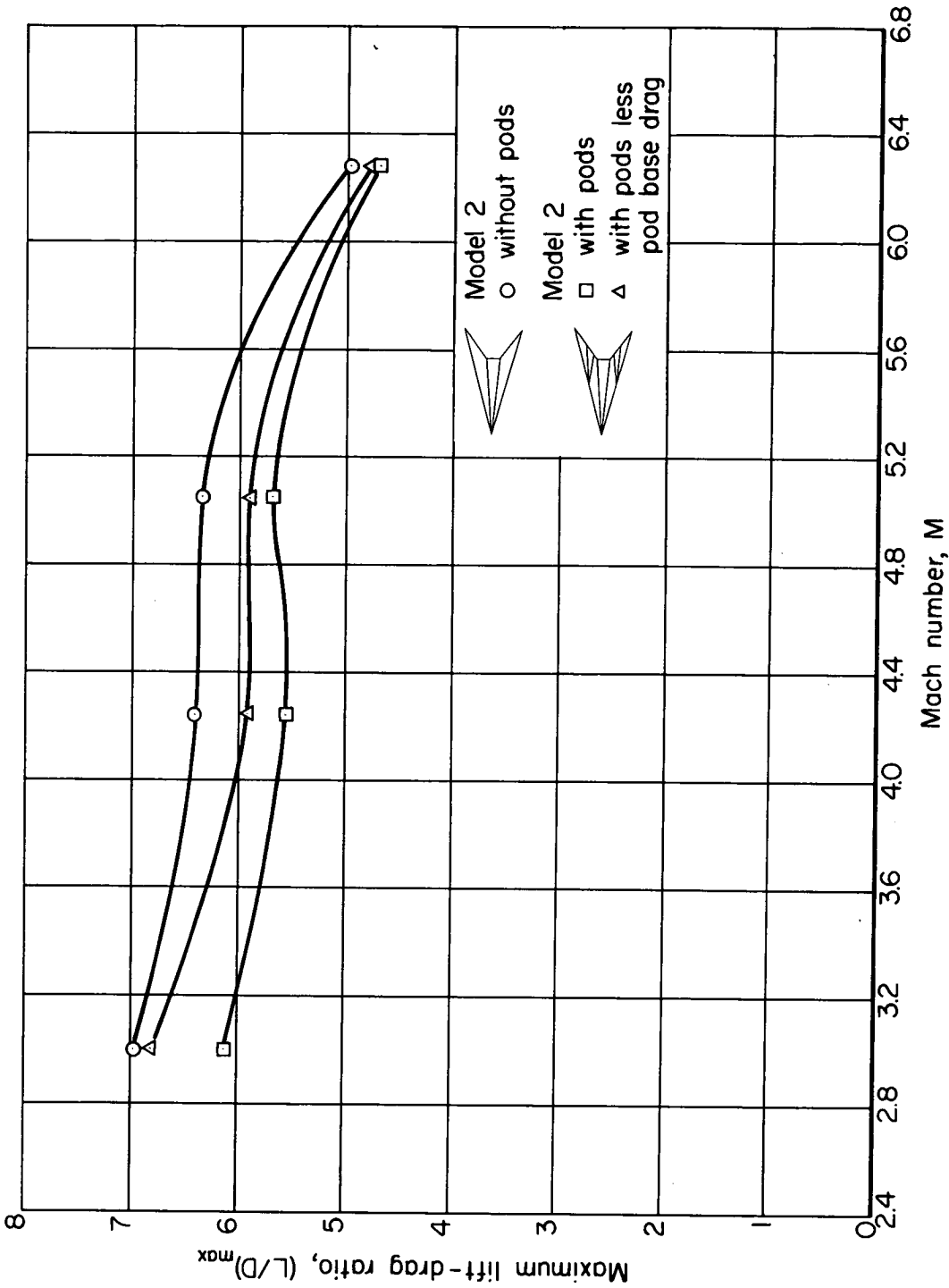


Figure 5.- Effect of the addition of auxiliary bodies on maximum lift-drag ratios.

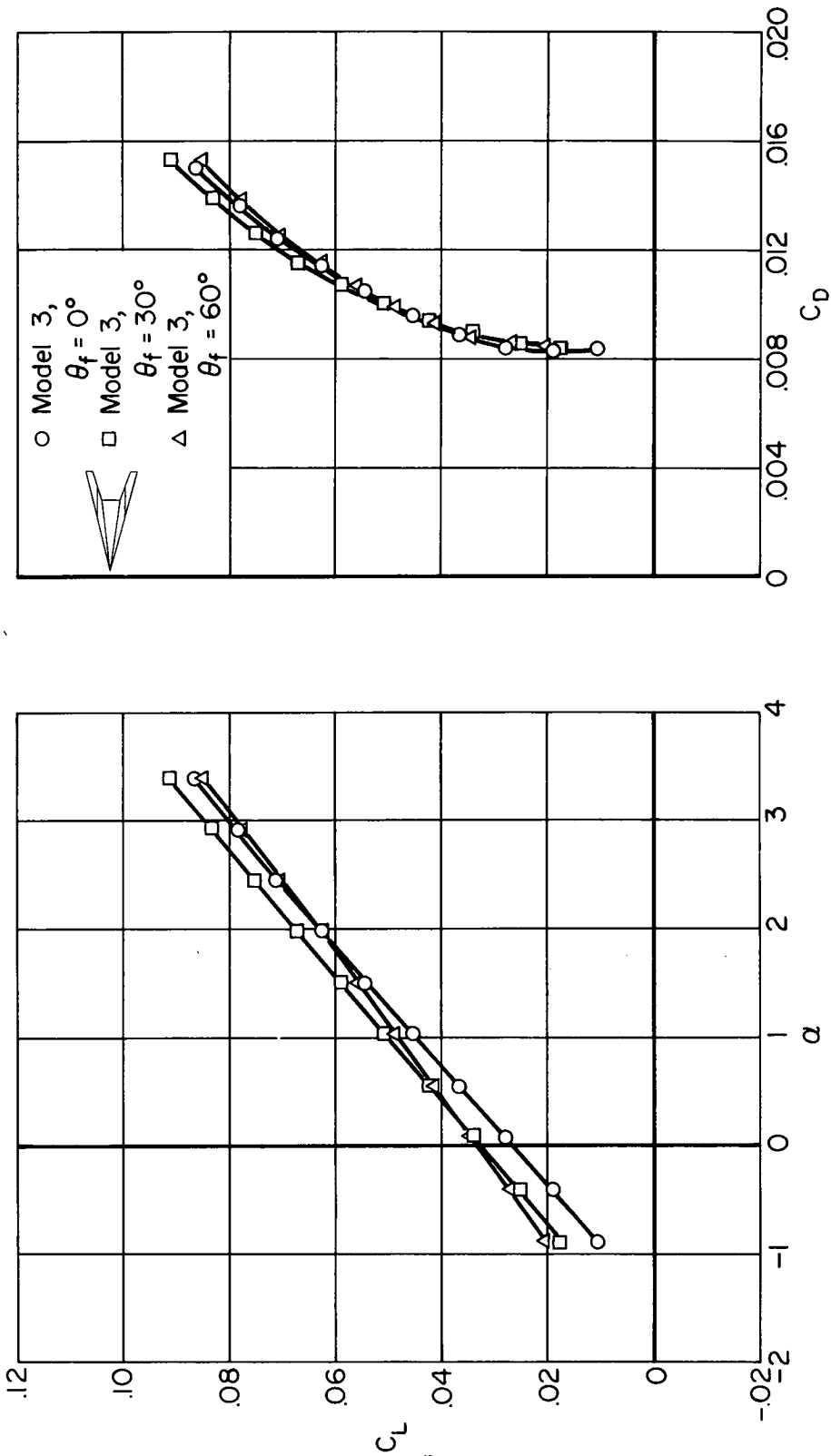
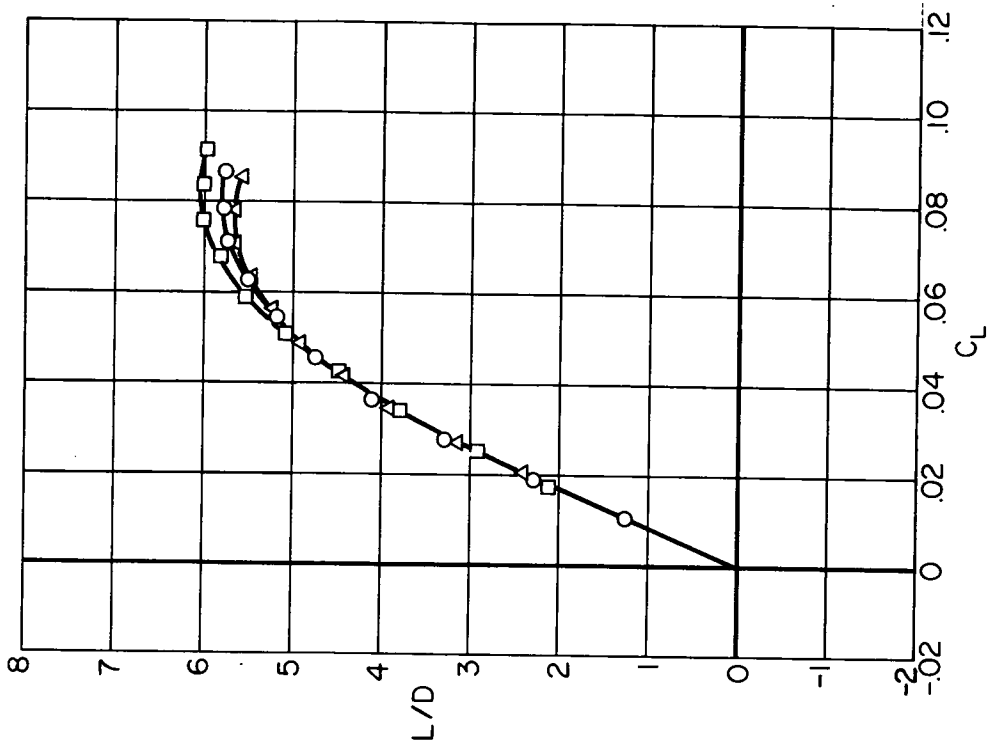
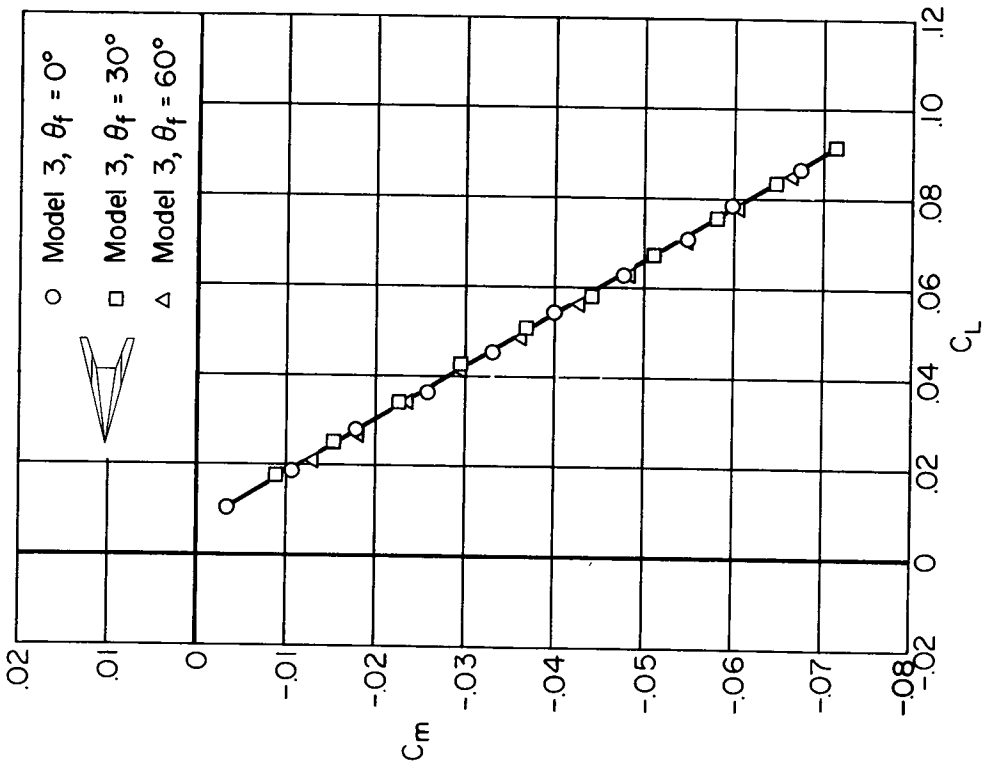


Figure 6.- Effect of tip-flap deflection on the aerodynamic characteristics of flat-top wing-body combinations at M = 5.05.



(d) Lift-drag ratio.



(c) Longitudinal stability.

Figure 6.- Concluded.

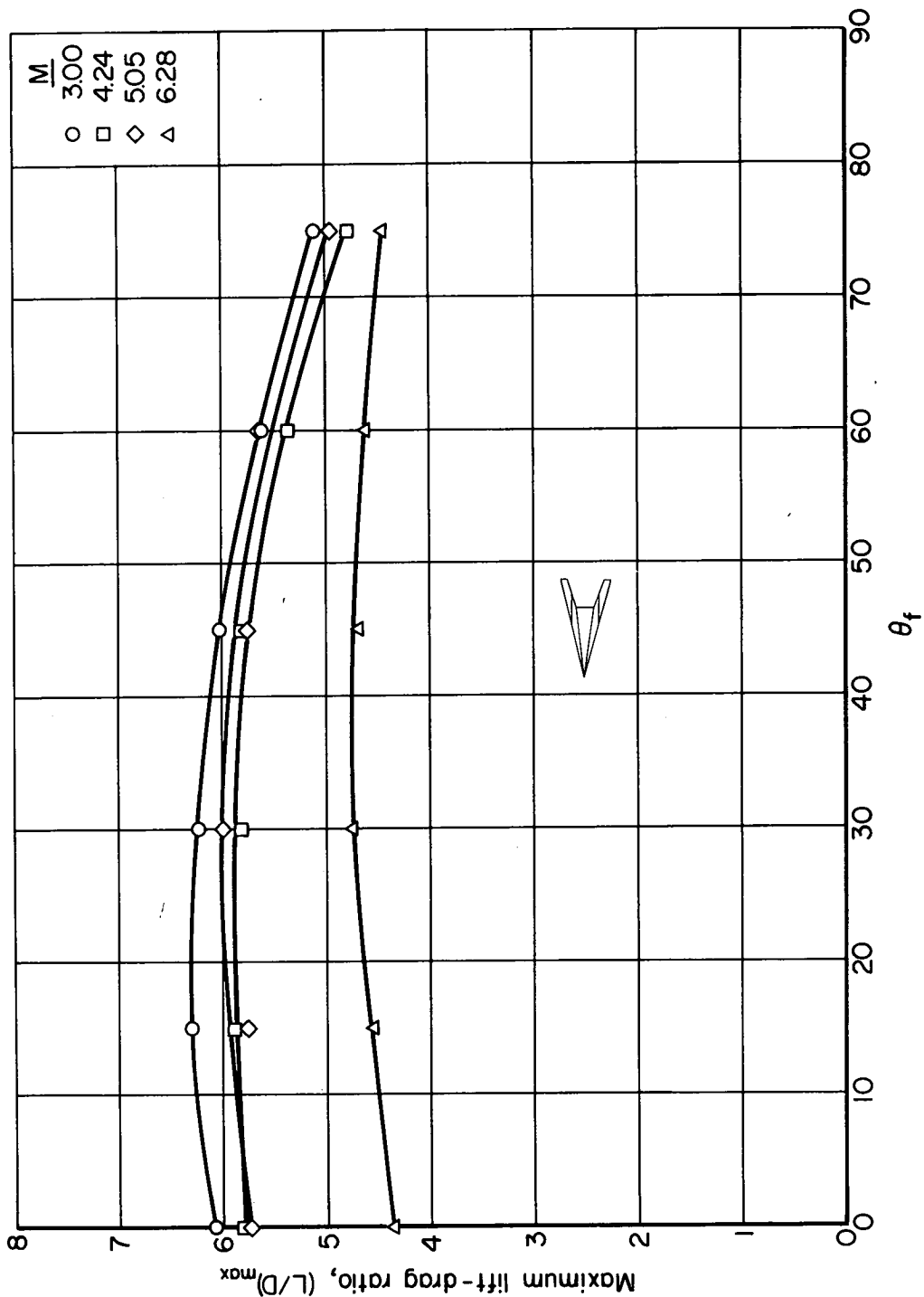


Figure 7.- Effect of tip-flap deflection on maximum lift-drag ratios (Model 3).

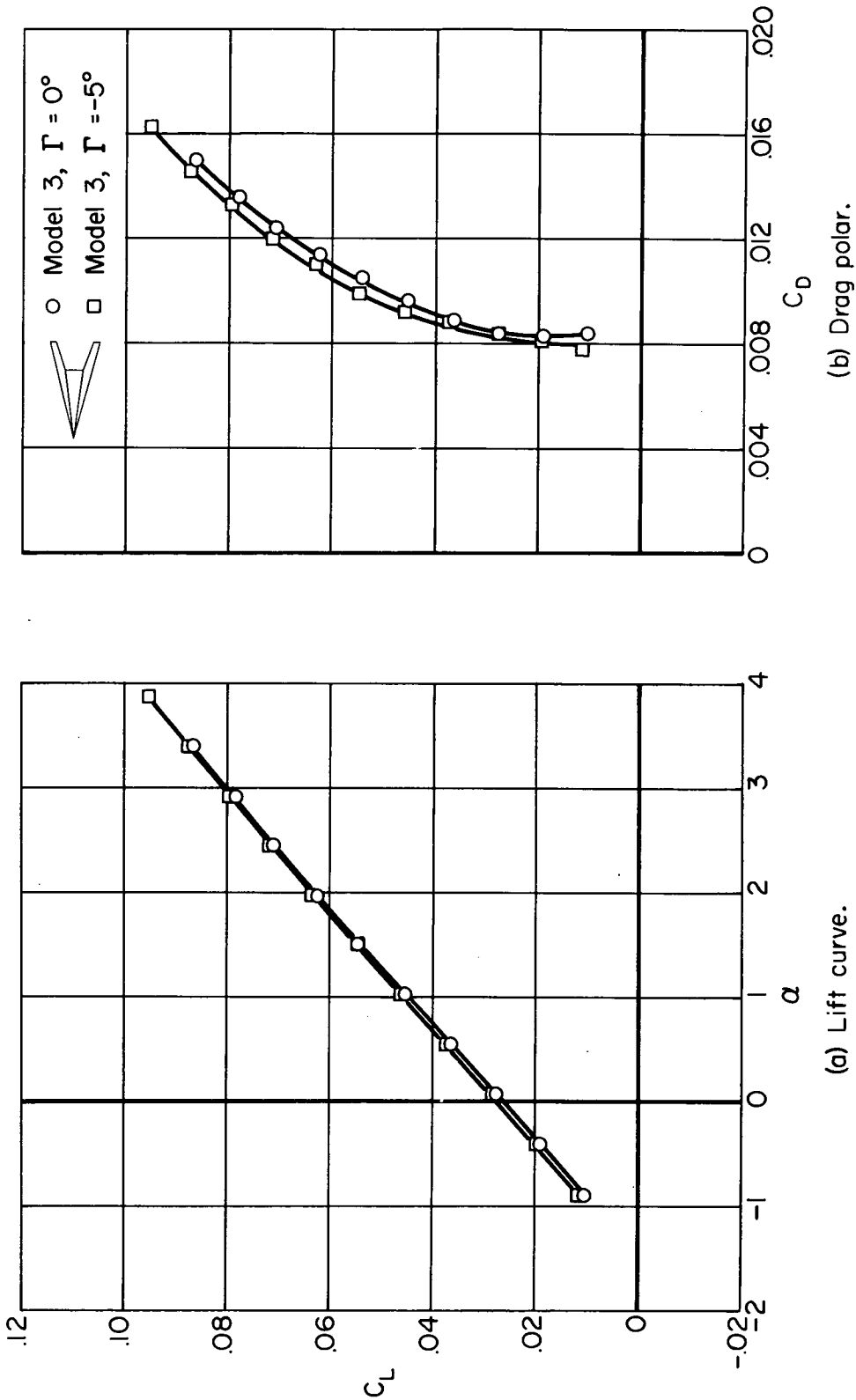
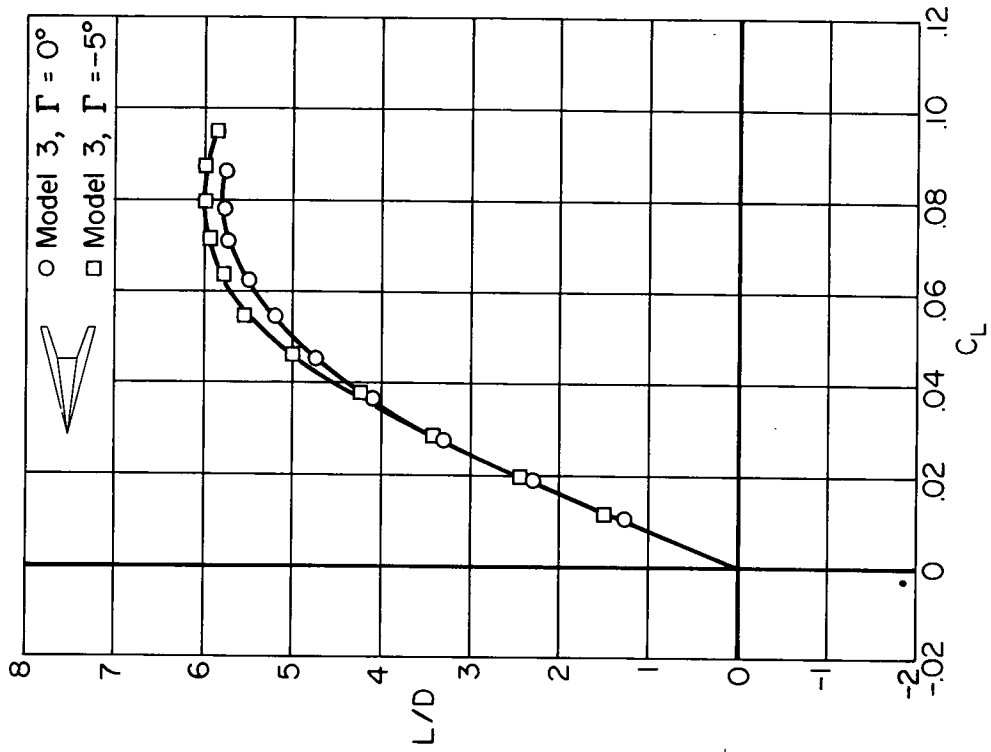
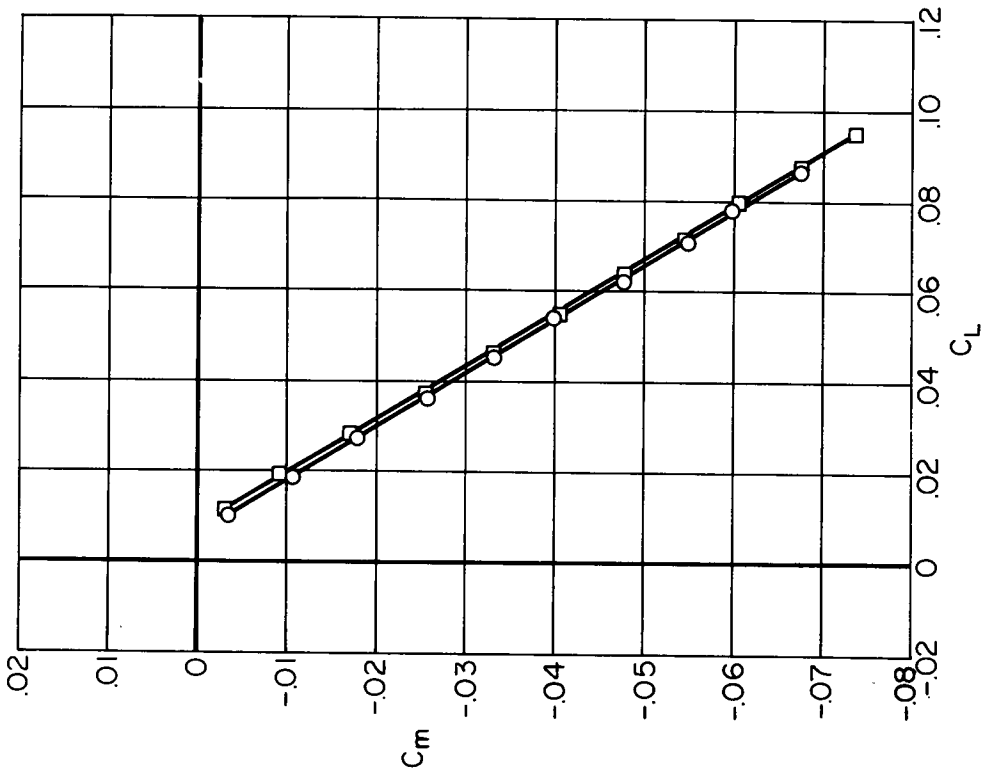


Figure 8.- Effect of dihedral on the aerodynamic characteristics of flat-top wing-body combinations at  $M = 5.05$ .



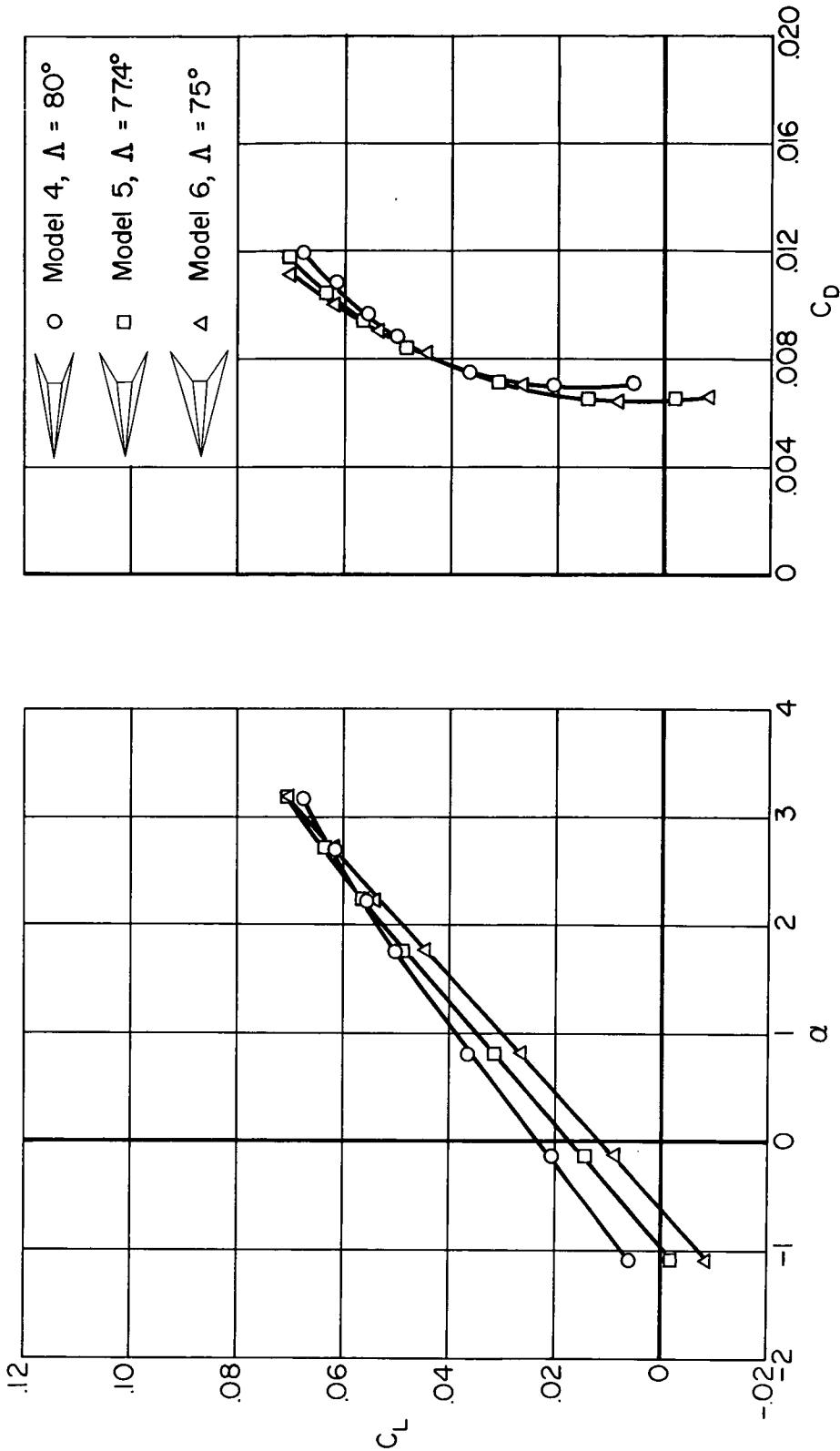
(d) Lift-drag ratio.



(c) Longitudinal stability.

Figure 8.- Concluded.





(a) Lift curve.

(b) Drag polar.

Figure 9.- Effect of leading-edge sweep on the aerodynamic characteristics of flat-top wing-body combinations at  $M = 5.05$ .

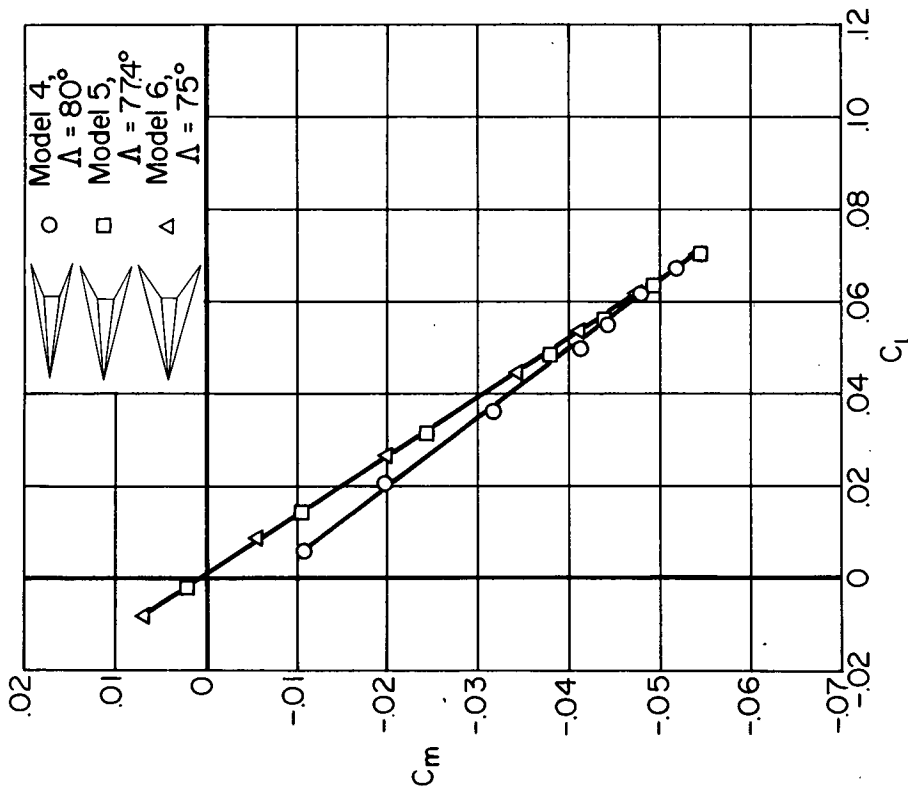
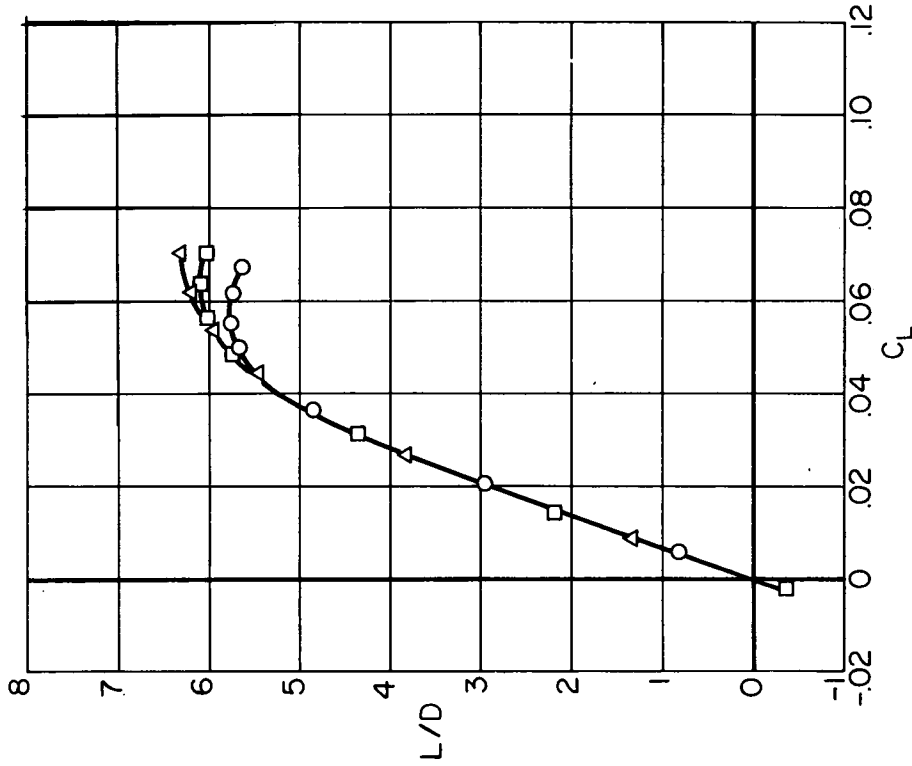
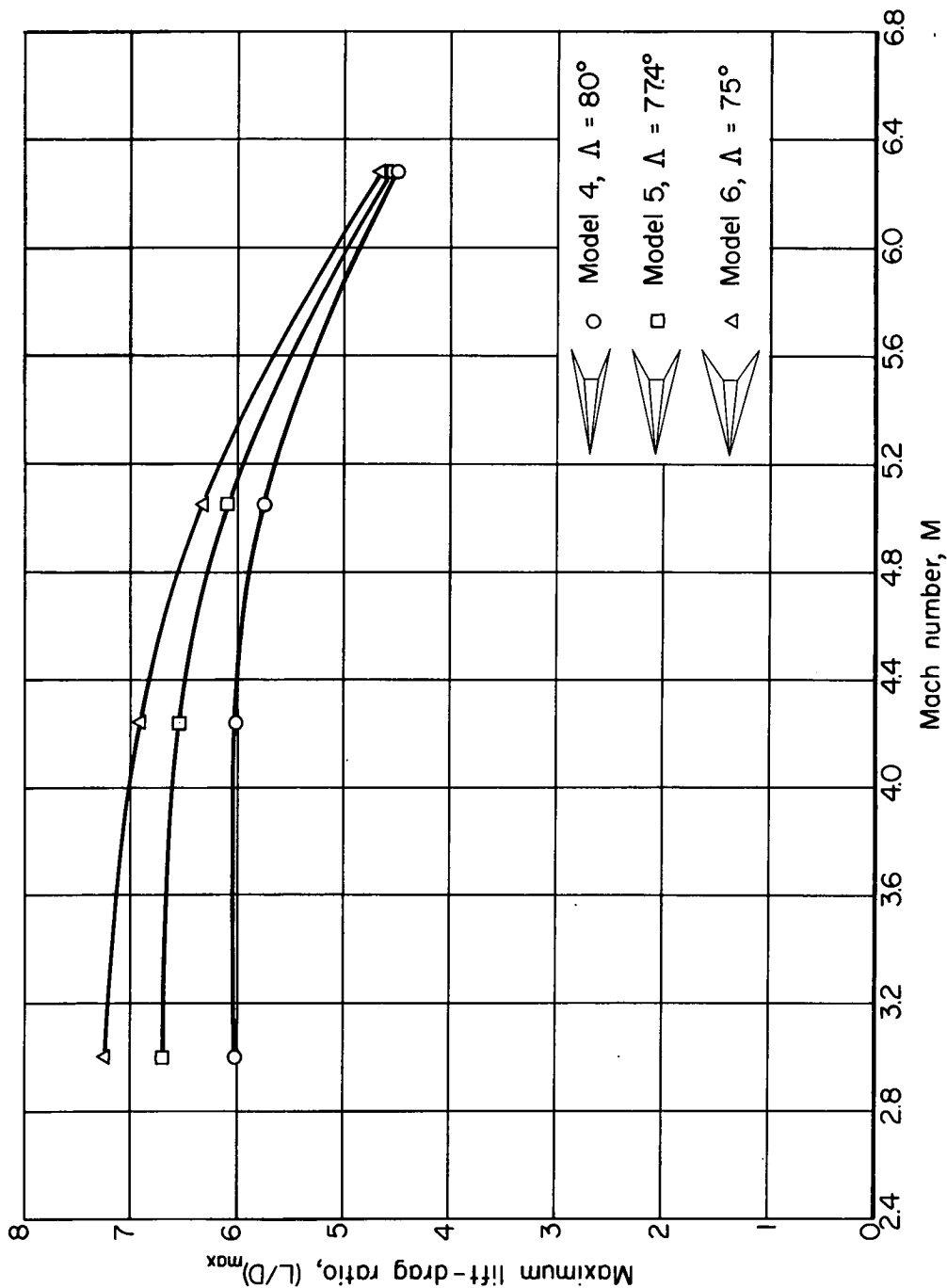
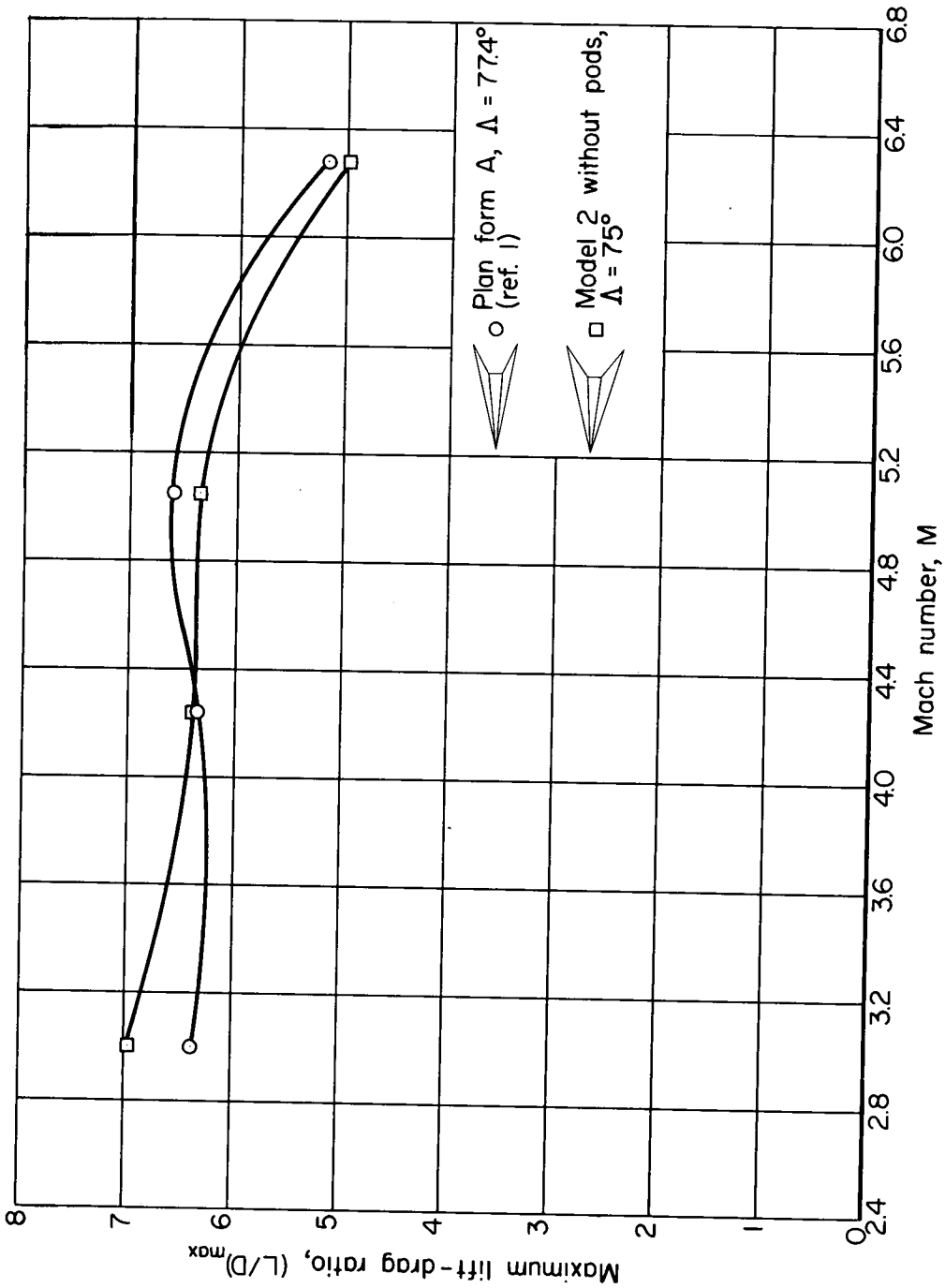


Figure 9.- Concluded.



(a) Fuselage semivertex angle,  $\delta_c = 5.71^\circ$ .

Figure 10.- Effect of leading-edge sweep on maximum lift-drag ratios.



(b) Fuselage semivertex angle,  $\delta_c = 5.00^\circ$

Figure 10. - Concluded.

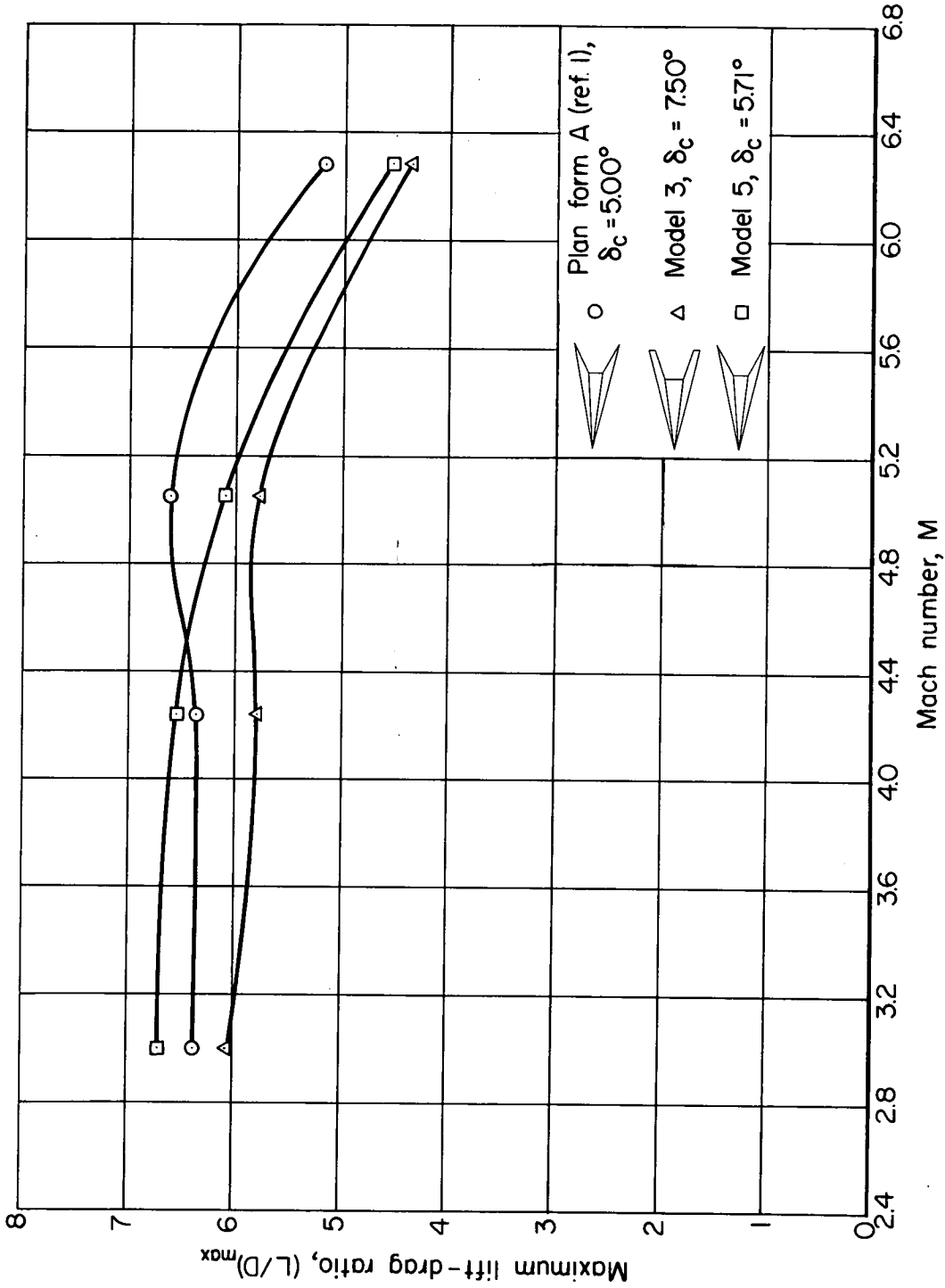
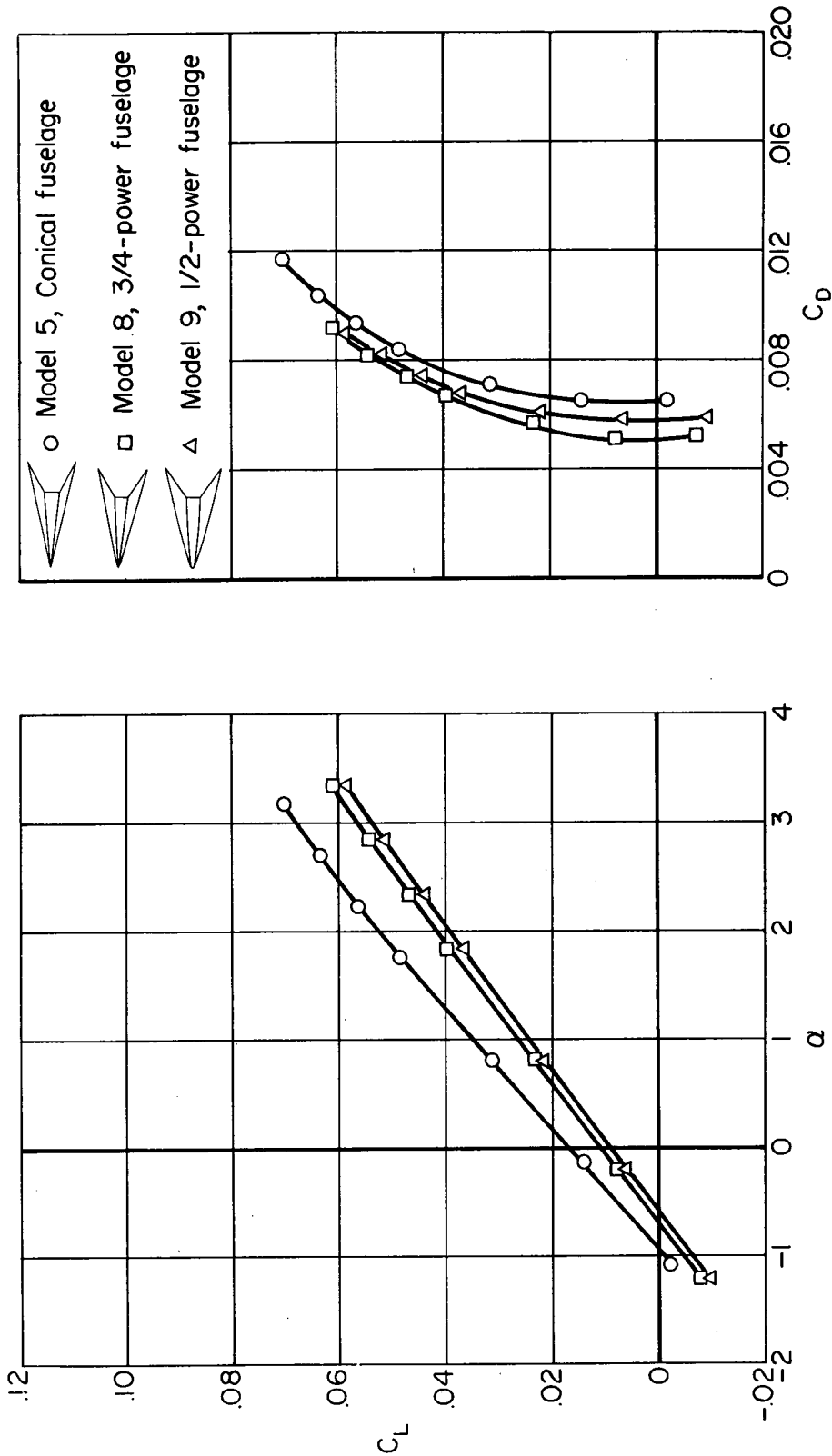


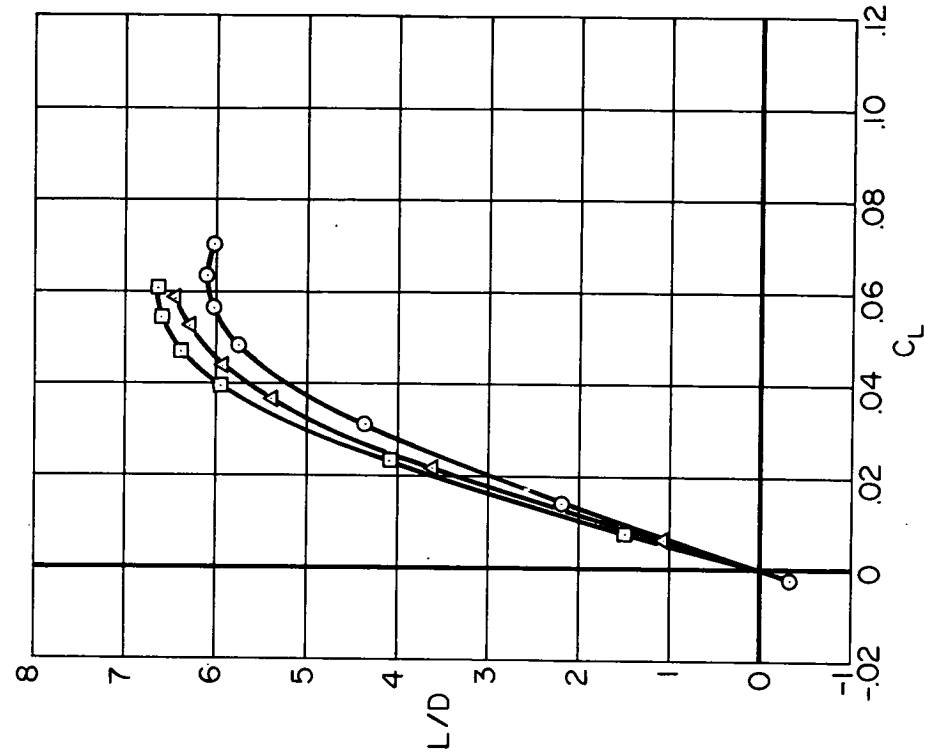
Figure 11.- Effect of fuselage fineness ratio on maximum lift-drag ratios.



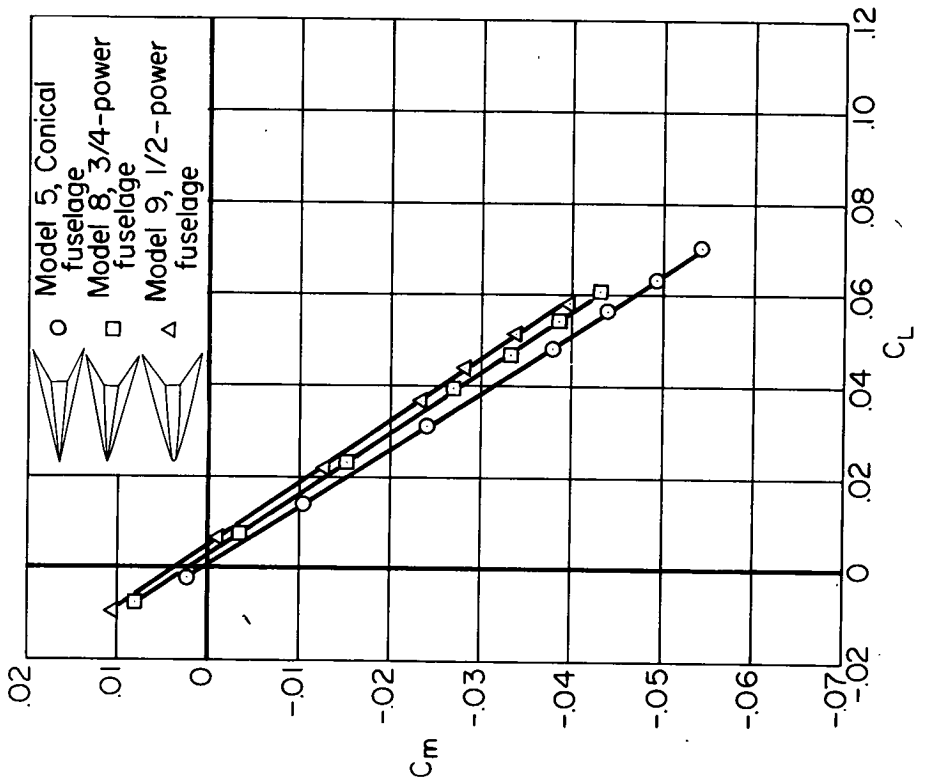
(a) Lift curve.

(b) Drag polar.

Figure 12.- Effect of fuselage shape on the aerodynamic characteristics of flat-top wing-body combinations at  $M = 5.05$  (Models 5, 8, and 9).



(d) Lift-drag ratio.



(c) Longitudinal stability.

Figure 12.- Concluded.

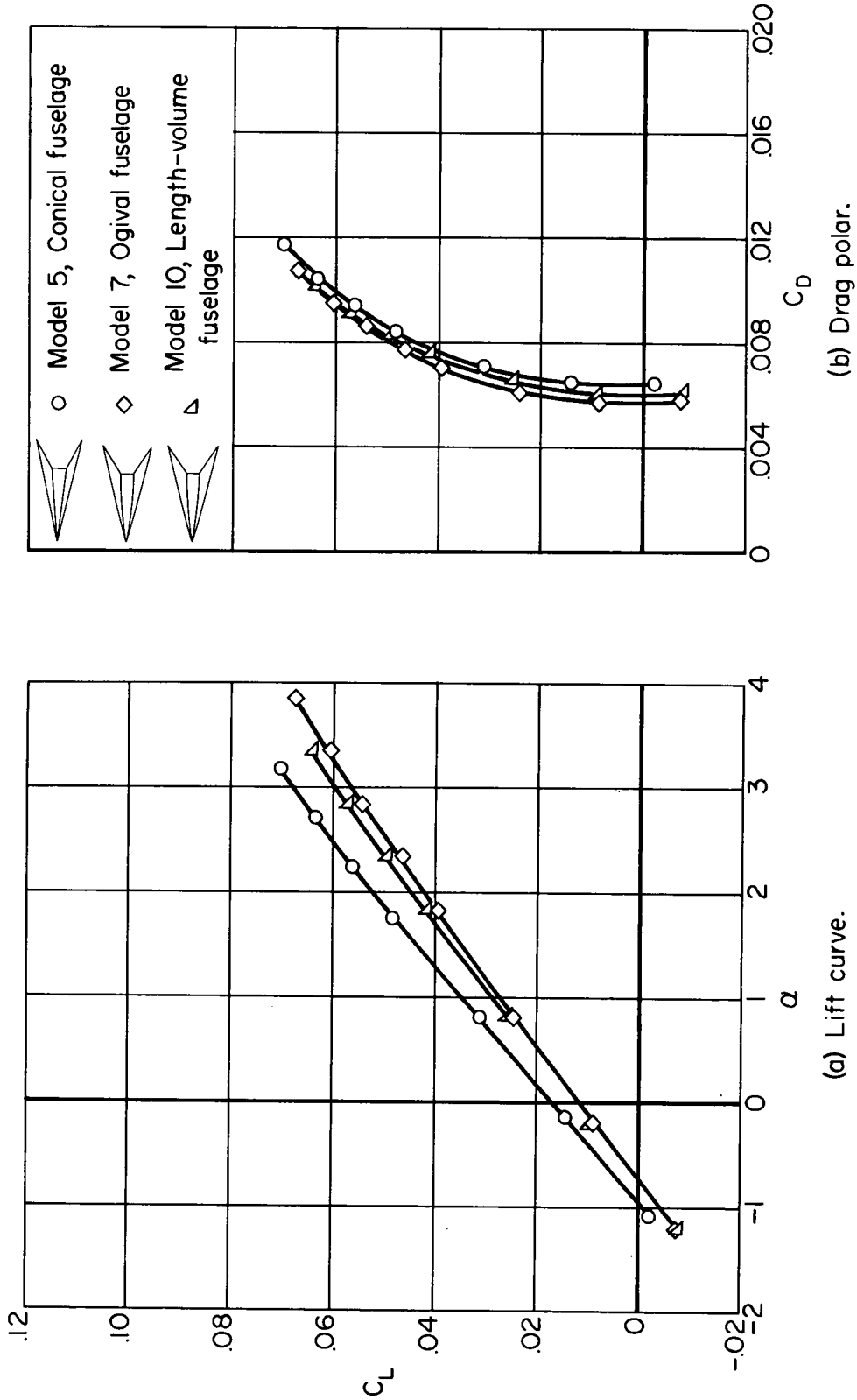
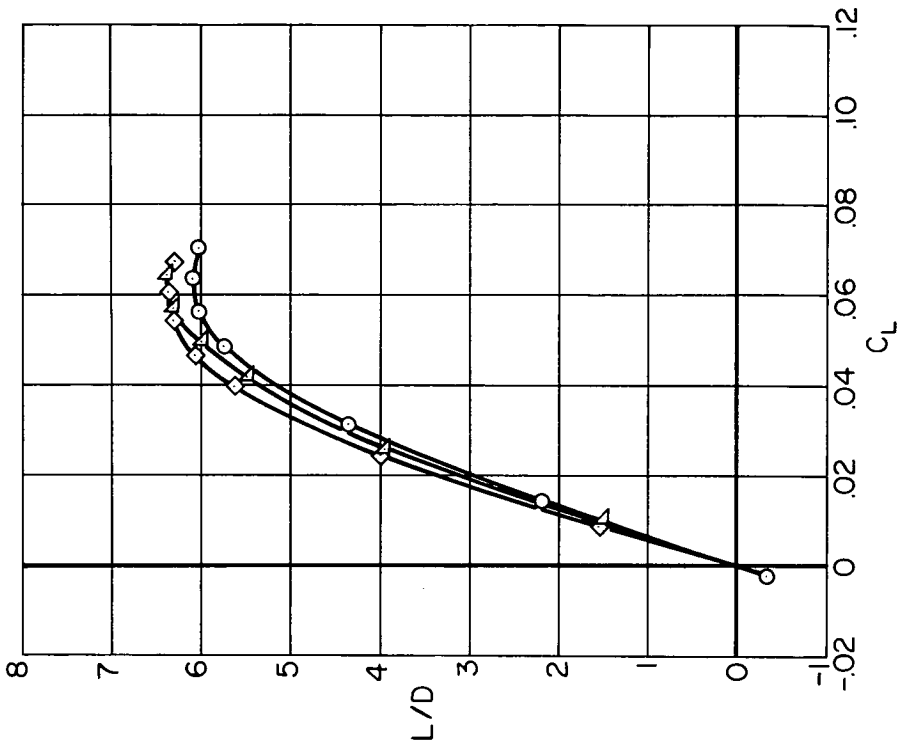
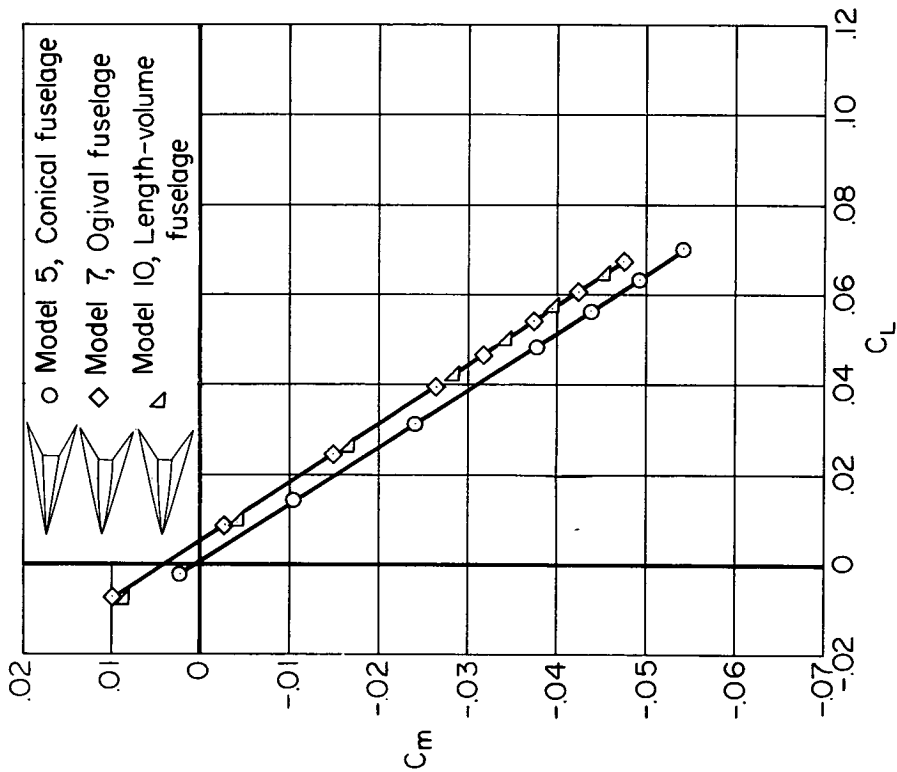


Figure 13.- Effect of fuselage shape on the aerodynamic characteristics of flat-top wing-body combinations at  $M = 5.05$  (Models 5, 7, and 10).





(d) Lift-drag ratio.



(c) Longitudinal stability.

Figure 13.- Concluded.

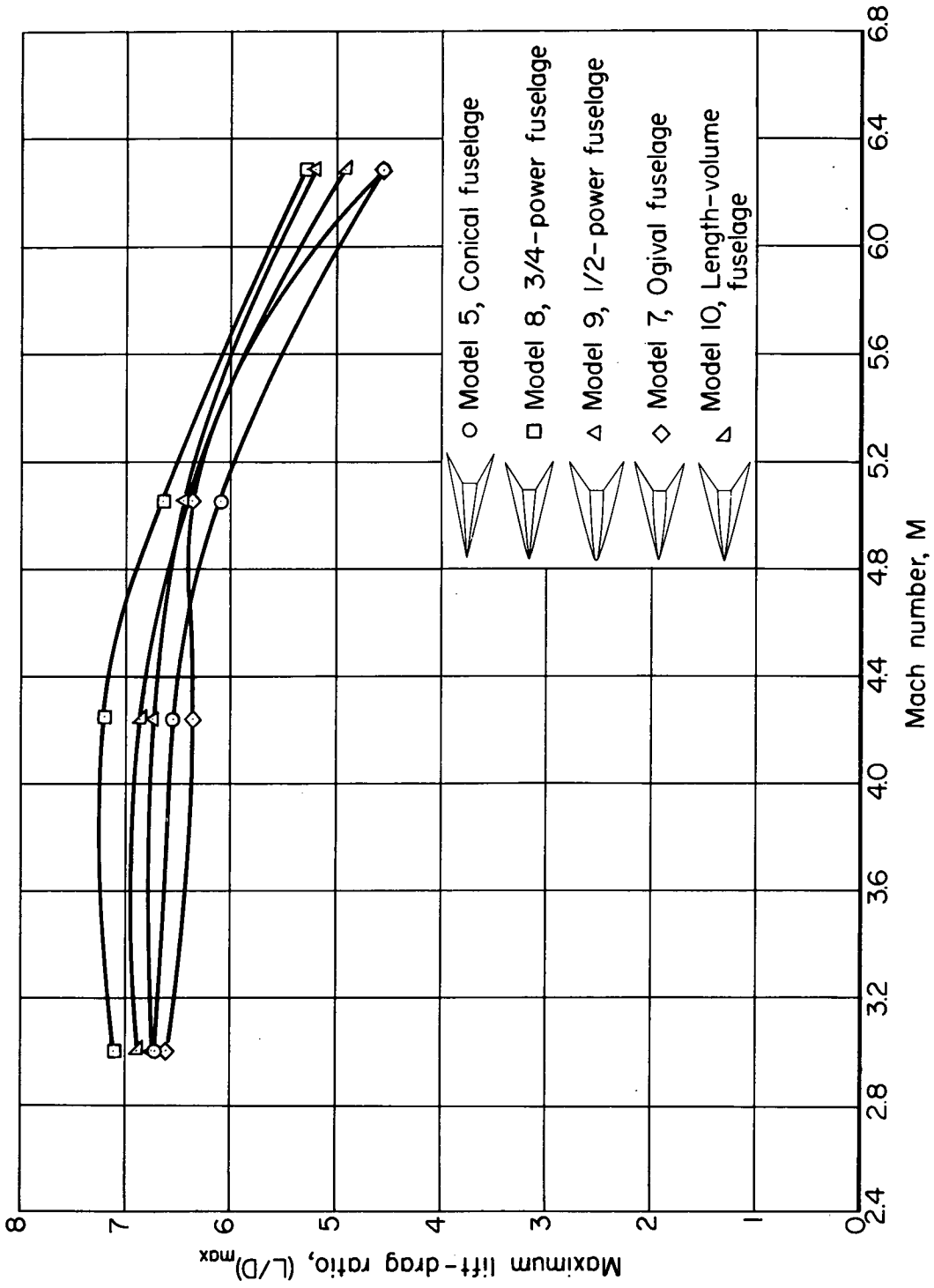


Figure 14.- Effect of fuselage shape on maximum lift-drag ratios.

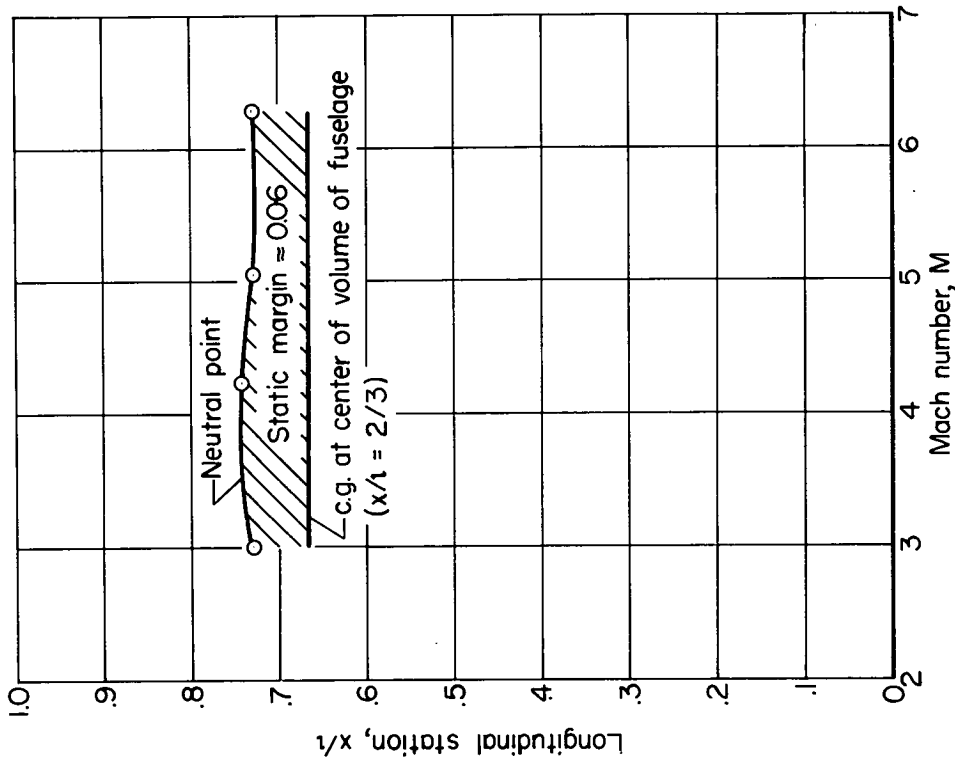
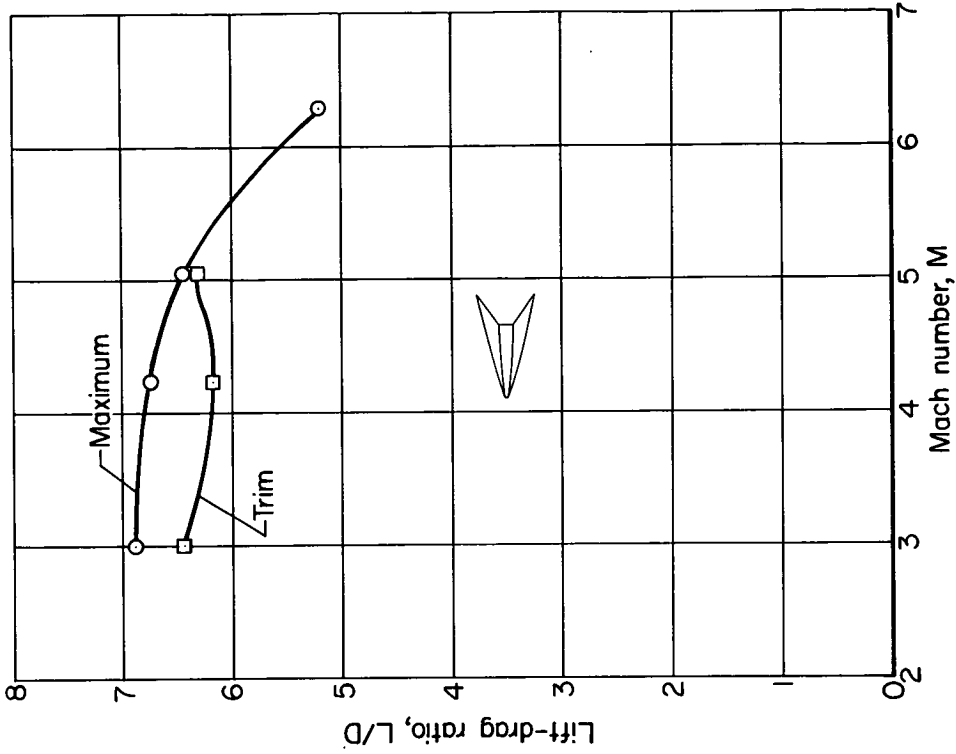


Figure 15.- Self-trimming characteristics of flat-top configuration with 1/2-power fuselage (Model 9).

DECLASSIFIED

CONFIDENTIAL

ALL INFORMATION CONTAINED  
HEREIN IS UNCLASSIFIED  
DATE 08/14/01 BY 60322 UCBAW

CONFIDENTIAL